PHILOSOPHICAL TRANSACTIONS OF THE ROYAL SOCIETY A MATHEMATICAL, PHYSICAL & ENGINEERING SCIENCES

The Influence of High Pore-Water Pressure on the Strength of Cohesionless Soils

A. W. Bishop and A. E. Skinner

Phil. Trans. R. Soc. Lond. A 1977 **284**, 91-130
doi: 10.1098/rsta.1977.0001

THE INFLUENCE OF HIGH PORE-WATER PRESSURE ON THE STRENGTH OF COHESIONLESS SOILS

By A. W. Bishop and A. E. Skinner
Civil Engineering Department, Imperial College of Science and Technology, South Kensington, London SW7 2BU

(*Communicated by A. W. Skempton, F.R.S. – Received* 12 *August* 1975 – *Diagrams for reproduction received* 8 *March* 1976)

[Plate 1]

CONTENTS

The influence on the mechanical properties of saturated particulate materials of the component of stress carried by the water filling the pore space is fundamental to both theoretical and experimental studies in soil mechanics.

The rôle of pore pressure in controlling compressibility and shear strength is expressed in Terzaghi's *principle of effective stress* to a degree of accuracy which is sufficient for most engineering purposes. However, the precise significance of the small but finite area of interparticle contact has remained uncertain in the application of this equation to shearing resistance.

In the present paper the possible errors associated with the use of current expressions for intergranular stress and effective stress are examined. These errors are of significant magnitude at high values of pore pressure and low values of the yield stress of the solid forming the particles. A very accurate experimental investigation has been carried out into the sensitivity of shearing resistance to large changes in pore pressure (up to 41.4 MN/m²), using particulate materials ranging in strength from Quartz sand to lead shot.

The results indicate that the simple Terzaghi effective stress equation $\sigma' = \sigma - u$ is consistent with all the observations, though for Quartz sand a range of pore pressure changes an order of magnitude higher is desirable for additional confirmatory evidence.

1. Introduction

During the five decades which have elapsed since Terzaghi (1923) first stated the principle of effective stress the physical basis of the principle and the equations used to express it have been the subject of periodic review and occasionally of lively controversy. Throughout this period there has been a tendency to ignore the intention underlying Terzaghi's definition of effective stress and to identify effective stress with intergranular stress (for example Bruggeman, Zangar & Brahtz 1939; Taylor 1944, 1948; Scott 1963). While the consequent error is small for the relatively low values of pore pressure and interparticle contact area usually encountered in engineering practice, significant errors arise at the high values of pore pressure found in ocean bottom sediments, in oil and gas reservoirs and in various geophysical studies. Likewise in concrete and rocks, where the area of contact is large even at low stresses, the use of a correct effective stress equation is particularly important.

Terzaghi (1936) restated the principle of effective stress in the following terms (in current terminology):

'The stresses at any point of a section through a mass of soil can be computed from the *total principal stresses* σ_1, σ_2, σ_3 which act in this point. If the voids of the soil are filled with water under a stress u, the total principal stresses consist of two parts. One part, u, acts in the water *and* in the solid in every direction with equal intensity. It is called the *neutral stress* (or pore-water pressure). The balance $\sigma'_1 = \sigma_1 - u$, $\sigma'_2 = \sigma_2 - u$ and $\sigma'_3 = \sigma_3 - u$ represents an excess over the neutral stress u and has its seat exclusively in the solid phase of the soil.'

'This fraction of the total principal stresses will be called the *effective principal stresses*.... A change in the neutral stress u produces practically no volume change and has practically no influence on the stress conditions for failure.... Porous materials (such as sand, clay and concrete) react to a change in u as if they were incompressible and as if their internal friction were equal to zero. All the measurable effects of a change in stress, such as compression, distortion and a change in shearing resistance are exclusively due to changes in the effective stresses σ'_1, σ'_2, σ'_3. Hence every investigation of the stability of a saturated body of soil requires the knowledge of both the total and the neutral stress'.

It will be noted that in this statement the emphasis is on the exclusive relation between all the measurable effects of a change in stress (compression, distortion and a change in shearing resistance) and changes in the effective stresses σ'_1, σ'_2, σ'_3. Terzaghi's simple expression for effective stress

$$\sigma' = \sigma - u \tag{1}$$

has been shown (Bishop & Eldin 1950; Bishop 1955; Skempton 1960) to hold rigorously for the case of volume change if the two conditions in the statement quoted are put in the form

(1) the soil grains are incompressible,

(2) the yield stress of the grain material, which controls the contact area and intergranular shearing resistance, is independent of the confining pressure (as in the theories of friction due to Terzaghi (1925) and Bowden & Tabor (1942)).

It was also inferred by Bishop (1955) and demonstrated more rigorously by Skempton (1960) that the simple expression for effective stress $\sigma' = \sigma - u$ should hold for changes in shear strength if condition (2) were satisfied.

Actual soils do not fully satisfy either condition. Skempton (1960) has examined the significance

of the departures from both conditions (1) and (2) and has derived modified expressions for effective stress. In the next section the various expressions for effective stress and intergranular stress will be briefly presented and discussed.

2. Expressions for intergranular stress and effective stress

(*a*) *Intergranular stress*

It has been considered by a number of investigators that, *a priori*, the mechanical behaviour of a particulate mass is controlled by the forces acting at the particle-to-particle contacts. Taylor (1948, p. 126) states: 'In concepts of stresses ... the surface that must be considered is the one containing the points of grain-to-grain contact, in order that it may include the points of action of the forces which make up intergranular stress. Thus the unit area should be visualized as a wavy surface which is tangent to but does not cut through soil grains, and which at all points is as close as possible to a flat surface.'

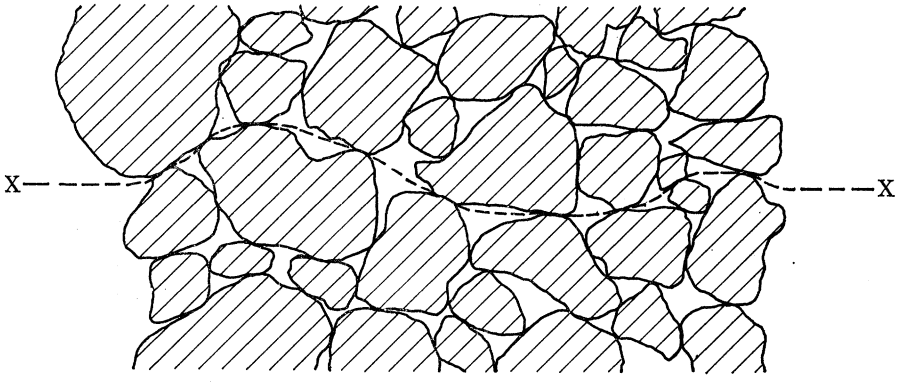

Figure 1

Consideration of the equilibrium of the forces on such a flat surface (figure 1) leads to the relation between total stress σ, the intergranular stress σ_i (defined as the average intergranular force per unit area normal to the surface) and the pore-water pressure u

$$\sigma = \sigma_i + (1-a)u$$

or

$$\begin{aligned}\sigma_i &= \sigma - (1-a)\,u \\ &= (\sigma - u) + au, \end{aligned} \tag{2}$$

where a denotes the contact area of the soil particles per unit area of the surface (and projected onto the surface).

Taylor (1944) uses this expression in a discussion of the significances of pore pressure changes in undrained triaxial tests on Boston Clay and estimates the value of a on this basis, obtaining a value of about 3 %. Taylor suggested that the term 'neutral stress' should be applied to the product $(1-a)\,u$.

Most investigators have, however, agreed that a is small in cohesionless soils, and probably in clays, at the stress levels commonly encountered in engineering practice. Thus, provided u is of the same order of magnitude as $(\sigma - u)$ the term au may be neglected with little loss in accuracy. However, if u is very large compared with $(\sigma - u)$, the significance of the term au is radically

changed. For $u = 100(\sigma - u)$ a value of a of 1 % would lead to a product au equal in magnitude to $(\sigma - u)$ and a doubling of the magnitude of σ_i.

Since the magnitude of a cannot be measured directly and is a matter of some uncertainty in many soils, the validity or otherwise of the intergranular stress concept is clearly a matter of considerable importance.

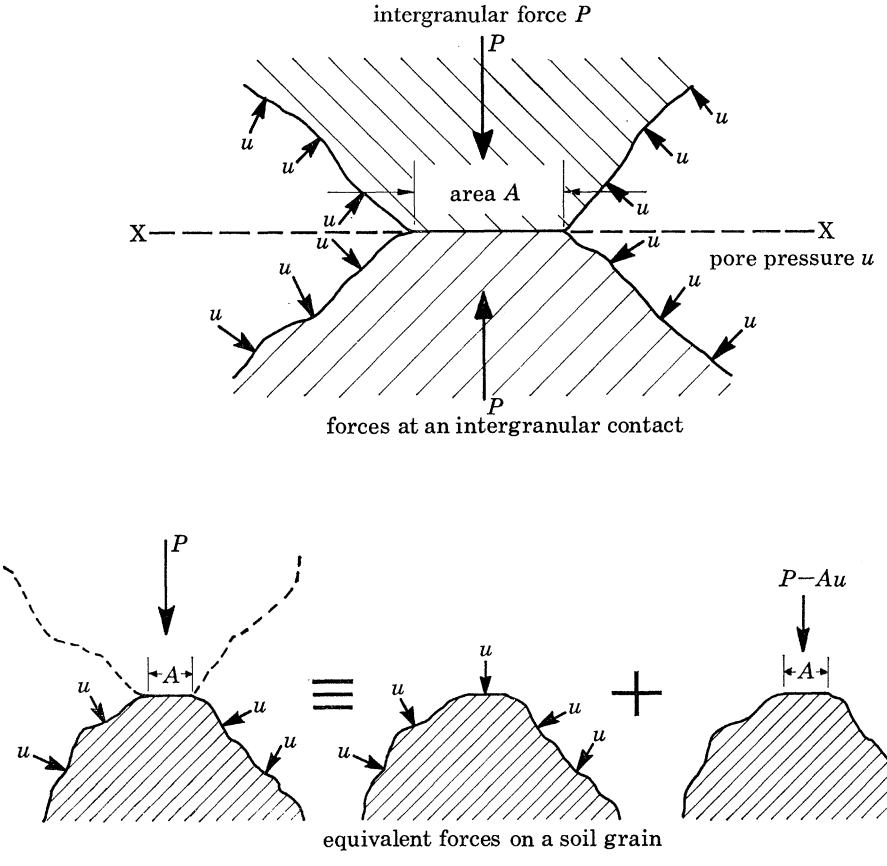

FIGURE 2

(*b*) *Effective stress for changes in volume*

Bishop & Eldin (1950) consequently examined the forces acting at an interparticle contact in the presence of pore-water under pressure (figure 2) and concluded that the distortion of the soil particle was not a function of the intergranular contact pressure, but of the excess of this pressure over the pore pressure acting on the adjacent surface of the particle. If the compressibility of the material comprising the soil particle was neglected as small compared with the bulk compressibility of the porous granular mass, then, irrespective of the magnitude of the interparticle contact area a, the equation for effective stress reduced to

$$\sigma' = \sigma - u.$$

Effective stress in this context† is defined as the function of total stress and pore pressure which controls volume change.

† The terminology used in the original paper by Bishop & Eldin (1950) reflected the current identification of the term effective stress with intergranular stress.

For this demonstration that the Terzaghi effective stress equation was independent of the magnitude of a, the two conditions stated in section (1) were necessary and sufficient.

The effect on the effective stress equation of a departure from condition (1), the incompressibility of the soil grains, was examined by Bishop (1953), who derived the expression

$$\sigma' = \sigma - (1 - C_s/C)\, u \qquad (3\,a)$$

or

$$\sigma' = (\sigma - u) + (C_s/C)\, u, \qquad (3\,b)$$

where C_s denotes the compressibility of the solid material forming the soil grains and C denotes the bulk compressibility of the porous mass for the relevant stress range.

For soils in the low stress range the bulk compressibility C is very large compared with the value of C_s. Skempton (1960) has tabulated data showing that for soils ranging from normally-consolidated clay to dense sand the ratio C_s/C lies in the range 0.00003–0.0015 for a consolidation pressure $(\sigma - u)$ of approximately 100 kN/m² (table 1). For a consolidation pressure of 20 MN/m² Skempton suggested that the ratio C_s/C is unlikely to exceed 0.01 in the case of clays. More recent test data from high pressure triaxial tests on London Clay (Bishop, Kumapley & El-Ruwayih 1975) indicate that at a consolidation pressure of 62.1 MN/m², C_s/C may rise to 0.04.

TABLE 1. (AFTER SKEMPTON 1960.)

(Compressibilities at $p = 1$ kg/cm²; water $C_w = 48 \times 10^{-6}$ per kg/cm²)

material	compressibility cm² kg⁻¹ C	compressibility cm² kg⁻¹ C_s	C_s/C
quartzitic sandstone	5.8×10^{-6}	2.7×10^{-6}	0.46
Quincy granite (100 ft deep)	7.5×10^{-6}	1.9×10^{-6}	0.25
Vermont marble	17.5×10^{-6}	1.4×10^{-6}	0.08
concrete (approx. values)	20×10^{-6}	2.5×10^{-6}	0.12
dense sand	$1\,800 \times 10^{-6}$	2.7×10^{-6}	0.0015
loose sand	$9\,000 \times 10^{-6}$	2.7×10^{-6}	0.000 3
London clay (over-cons.)	$7\,500 \times 10^{-6}$	2.0×10^{-6}	0.000 25
Gosport Clay (normally cons.)	$60\,000 \times 10^{-6}$	2.0×10^{-6}	0.000 03

Tests to examine the validity of the effective stress equation for volume change have been carried out by Laughton (1955) using high pore-water pressures in a sealed oedemeter. Laughton tested both lead shot, to ensure large values of interparticle contact area a which could be measured on unloading the sample, and Globigerina ooze from the bed of the eastern Atlantic ocean.

In both cases the test data demonstrate the validity (to within experimental error) of the effective stress equation $\sigma' = \sigma - u$, although in the case of the lead shot the observed value of a rose to 95 % at the highest effective stress (100 MN/m²). In a re-examination of the test data Skempton (1960) has shown that the effective stress equation (3) gives a marginally better fit in the case of lead shot when the value of C_s/C rises to 0.05 at the highest consolidation pressure.

Skempton (1960) also examined the consequence of a departure from condition (2) on the effective stress equation for volume change and found it to be numerically unimportant in most cases.

It is of interest to note that, since the bulk properties of a granular mass subject to a change in stress are not those of an ideal elastic material, the value of C is not a unique parameter for a particular soil (as is C_s) but depends on the stress level, the previous stress path, the sign and magnitude

of the stress change, and the rate of loading (Bishop & Blight 1963). Furthermore, although effective stress as defined by equation (3) determines the overall volume change, it is the component $\sigma - u$ which determines the change in compressibility C (Bishop 1973).

While it is apparent from the preceding discussion that the more rigorous expression for effective stress with respect to volume change need only be used for soils at very high consolidation pressures, for concrete and for porous rocks the term C_s/C is of much greater significance even in the low stress range. Data presented by Skempton (1960) indicate values of C_s/C of around 0.12 for concrete and from 0.08 to 0.46 for various rocks (table 1).

(*c*) *Effective stress for changes in shear strength*

Terzaghi (1936) considered that the same effective stress equation $\sigma' = \sigma - u$ applied equally to both changes in volume and to changes in shear strength.

Bishop (1955) considered that, if an analogy could be drawn between interparticle friction and metallic friction, then the contact area would control the frictional forces and this area, like the deformation of the soil particles, would be controlled by σ' $(= \sigma - u)$. Hence it might be inferred that the expression for effective stress $\sigma' = \sigma - u$ would be valid for shear strength irrespective of contact area, provided condition (2) was satisfied.

Skempton (1960) presented a formal analysis of interparticle friction in the presence of pore water under pressure, arriving at the same conclusion for the special case represented by condition (2), but also extending the analysis to include the more general case of grain materials whose strength is a function of confining pressure of the form:

$$\tau_i = k + \sigma \tan \psi, \tag{4}$$

where τ_i denotes shear stress at failure, σ denotes normal stress, k denotes intrinsic cohesion, and ψ denotes the angle of intrinsic friction of the solid.

For these materials Skempton obtained an expression for effective stress with respect to change in shear strength:

$$\sigma' = \sigma - \left(1 - \frac{a \tan \psi}{\tan \phi'}\right) u \tag{5a}$$

$$= (\sigma - u) + au \frac{\tan \psi}{\tan \phi'}, \tag{5b}$$

where a denotes interparticle contact area, as before, and ϕ' denotes the angle of shearing resistance of the granular mass (in terms of effective stress).

Skempton (1960) examined published test data from jacketed and unjacketed triaxial tests on Marble and Solenhofen Limestone and concluded that the areas of contact given by equation (5) (0.15 and 0.45 respectively) were consistent with the changes in strength with confining pressure obtained with the jacketed samples. He also concluded that area of contact deduced from concrete was about 0.2, and, though not subject to any independent check, was not unreasonable. For soils no critical test data was available, and Skempton concluded that Terzaghi's equation would be a valid approximation due to the small value of a.

In deriving equation (5) Skempton assumed that there is a direct relation between ϕ', the angle of shearing resistance of a non-cohesive granular material, and μ, the coefficient of friction at an interparticle contact, quoting the expression due to Caquot (1934) for constant volume shear:

$$\tan \phi' = \tfrac{1}{2}\pi\mu. \tag{6}$$

Similar though not identical relations have been obtained by Bishop (1954) and Horne (1969), but involve simplifying physical assumptions and, in the case of the earlier expression, a mathematical approximation.

This form of relation is, however, not supported by a series of very careful tests carried out by Skinner (1969, 1975) on particles of almost identical shape but of widely differing values of the coefficient μ (figure 3). Skinner's results are supported by independent tests carried out on rock fragments and gravel by Tombs (1969) and discussed by Bishop (1969).†

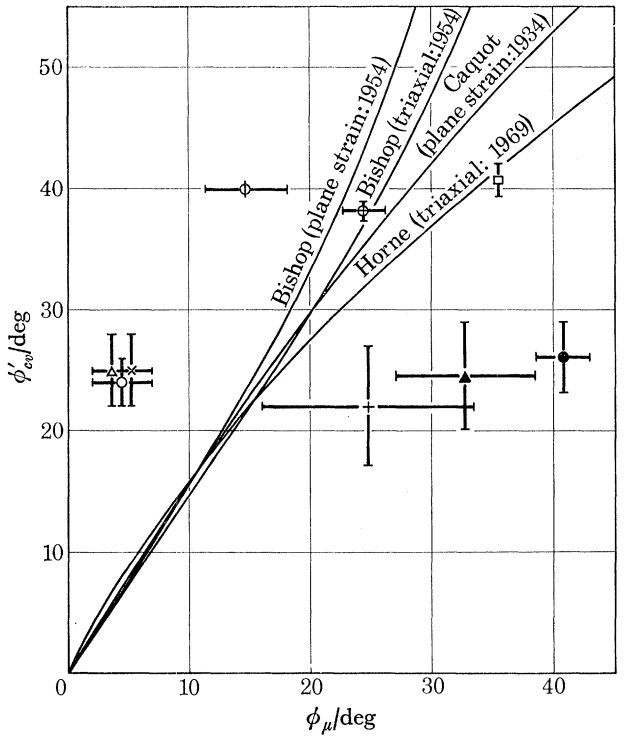

△ 1 mm diam. glass ballotini (dry)
▲ 1 mm diam. glass ballotini (flooded)
○ 3 mm diam. glass ballotini (dry)
● 3 mm diam. glass ballotini (flooded)
\+ $\frac{1}{8}$ in. diam. steel ball bearings (dry)
× 3 mm diam. lead shot (dry)
} shear box tests after Skinner (1969)

ϕ chert
⊕ mudstone
□ granite
} Rockfill triaxial tests after Tombs (1969)

FIGURE 3. Theoretical and experimental relations between ϕ_μ and ϕ_{cv} (Skinner 1969).

Lack of direct relation between ϕ' and μ is associated with the complexity of particle movement in a particulate mass subject to a shear strain, which involves not only interparticle slip but particle rotation and out-of-plane displacements even under an overall plane strain displacement.‡ It suggests, furthermore, that one of the steps in the derivation of the effective stress

† Experimental support for the relation comes primarily from the tests in which μ has not in fact been measured directly and where its physical significance is open to serious criticism (see Horne 1969; Skinner 1969; Bishop 1969; Procter & Barton 1974).

‡ A detailed study using marked particles and X-ray stereo techniques has been carried out by Y. Sharma and is in course of preparation for publication.

equation (5) may be based on an assumption of doubtful validity, at least for cohesionless soils. This places added emphasis on the need for direct experimental verification of the effective stress equation for shear strength.

3. Testing programme, apparatus and testing techniques

The testing programme was designed generally to explore the influence of high pore-water pressures on the strength of cohesionless soils and in particular to discriminate between the intergranular and effective stress equations.

The difference between the three equations lies in the term involving the product au where the Terzaghi effective stress equation is

$$\sigma' = \sigma - u, \tag{1}$$

the intergranular stress equation is

$$\sigma_i = (\sigma - u) + au, \tag{2}$$

and Skempton's effective stress equation is

$$\sigma' = (\sigma - u) + mau, \tag{5}$$

where m is $\tan\psi/\tan\phi'$ and is of the order 0.3 for sand consisting of quartz particles and 0.03 for lead shot (Skempton 1960). The significance of the au term in influencing the strength, which, by definition, is controlled by σ', will depend on the magnitude of au relative to $(\sigma - u)$. In seeking, for reasons of experimental accuracy, to maximize the ratio r, where $r = au/(\sigma - u)$, we may note that, for a given particulate material, the magnitude of a depends almost linearly on $(\sigma - u)$ (Bishop & Eldin 1950; Skempton 1960). Hence we have

$$\begin{aligned} r &= \frac{au}{(\sigma - u)} \\ &= \frac{n(\sigma - u)\,u}{(\sigma - u)} \\ &= nu, \end{aligned} \tag{7}$$

where n is a constant depending on the strength parameters of the material. Thus the percentage difference in strength between the predictions of the three expressions will depend on the magnitude of the change in pore pressure (for $(\sigma - u)$ = constant), but will be independent of the actual magnitude of the consolidation pressure $(\sigma - u)$ and of the associated value of contact area a, depending instead on their ratio as represented by the parameter n. This means that the testing programme must involve the highest pore pressures (and consequently the highest cell pressures in the triaxial apparatus) consistent with the accurate measurement of small changes in strength, and must include materials in which the yield stress of the particles is relatively low.

The accurate measurement of small changes in strength at high cell pressures in the conventional triaxial apparatus is rendered almost impossible by (*a*) the friction on the loading ram and (*b*) the magnitude of the load due to the cell pressure acting on the inner end of the ram, this load being very large compared with that due to the strength change to be detected.

The error due to friction on the loading ram can be avoided by measuring the load inside the cell with an electric load transducer. However, the problem then arises of the sensitivity of the

transducer itself to large changes in cell pressure. As the purpose of the present series of tests was not merely to measure the strength changes correctly, but to demonstrate incontrovertibly that they had been measured correctly, the alternative method of rotating the bushing enclosing the loading ram was adopted (figure 4). Since the frictional force opposes the relative motion between the ram and the bushing, a rotary motion of about 2 rev/min is sufficient to reduce the vertical component of friction to negligible proportions at normal rates of axial displacement. The problems of excessive oil leakage and 'wobble' due to the loss of a common axis to the inner and outer cylindrical surfaces of the bushing during machining and honing call for a very high standard of workmanship in manufacture.

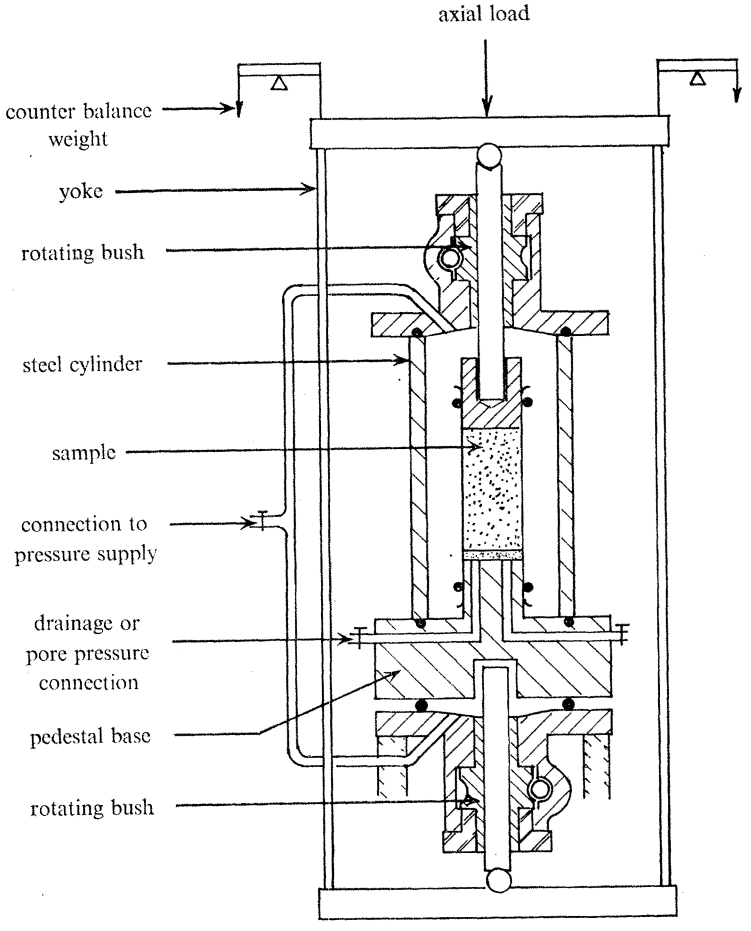

FIGURE 4

The relative magnitudes of the uplift on the end of the loading ram and the axial load required to shear the sample can be readily estimated for a maximum ratio of cell pressure σ_3 to consolidation pressure $\sigma_3 - u$ of *ca.* 100 and a ram to sample diameter ratio of $\frac{2}{3}$ (as used on the high pressure cell). From the geometry of the Mohr circle (figure 5) it follows that, for a cohesionless soil, the stress difference at failure (on the basis of the Terzaghi expression for effective stress) is given by the expression

$$(\sigma_1 - \sigma_3) = (\sigma_3 - u)\,\frac{2\sin\phi'}{1-\sin\phi'}. \qquad (8)$$

Hence, for a value of $\phi' = 35°$, the ratio of the axial load due to uplift to the axial load on the sample at failure (neglecting the area change during compression) is

$$\frac{\sigma_3 A_r}{(\sigma_1 - \sigma_3) A_s} = \frac{100 \times (\sigma_3 - u) \times 1.0^2 \times \pi}{(\sigma_3 - u) \times 2.69 \times 1.5^2 \times \pi},$$
$$= 16.5, \tag{9}$$

where A_r and A_s denote the cross-sectional areas of the ram and sample respectively.

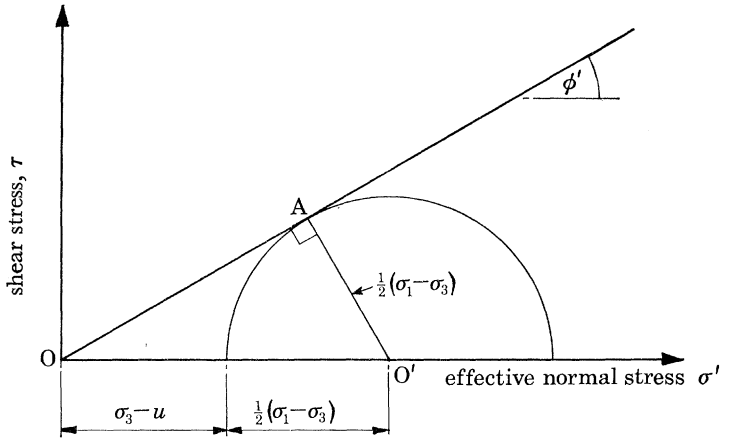

$$\sin\phi' = \frac{AO'}{OO'}, \text{ hence } \sigma_1 - \sigma_3 = (\sigma_3 - u)\frac{2\sin\phi'}{1-\sin\phi'}$$

FIGURE 5. The geometry of the Mohr diagram.

Thus to detect a change of 0.5 % in shear strength it would be necessary to measure the total axial load to an accuracy of 0.03 %, which is beyond the confidence limit of most load measuring devices.

The difficulty was resolved by balancing out hydraulically the load due to uplift with an opposed ram of identical diameter in a similar rotating bush (figure 4). A prototype triaxial cell was built (figure 6*a*, plate 1) mainly from components currently in use at Imperial College (Bishop, Webb & Skinner 1965) having a maximum cell pressure capacity of 6.9 MN/m² (1000 lbf/in²). With carefully matched rams (15.88 mm or 0.625 in nominal diameter) the maximum change in axial load for a change in cell pressure of 6.9 MN/m² was found to be 0.27 N (0.06 lbf) and was thus negligible relative to the load changes to be measured.

The success of the prototype led to the adoption of the same principle for a high pressure cell with a capacity of 69 MN/m² (10 000 lbf/in²). The technical problems to be overcome in actually manufacturing a rotating bush cell to operate in this pressure range were found to be formidable for three reasons in particular.

Firstly, the principle of rotating the bushing to eliminate the vertical component of friction was found to be ineffective if conventional oil seals were used. Hence control of the loss of the pressure fluid between the ram and the bushing depended solely on the length of the leakage path and the fineness of the fit. The length also necessitated a relatively stiff ram to avoid buckling in the higher load range. The dimensions chosen were a ram diameter of 25.4 mm (1.0 in) and an external bush diameter of 381 mm (1.5 in) with minimum and maximum radial clearances of 0.0038 and 0.0051 mm (0.00015 and 0.0002 in) internally and 0.0051 and 0.0064 mm (0.0002 and 0.00025 in) externally.

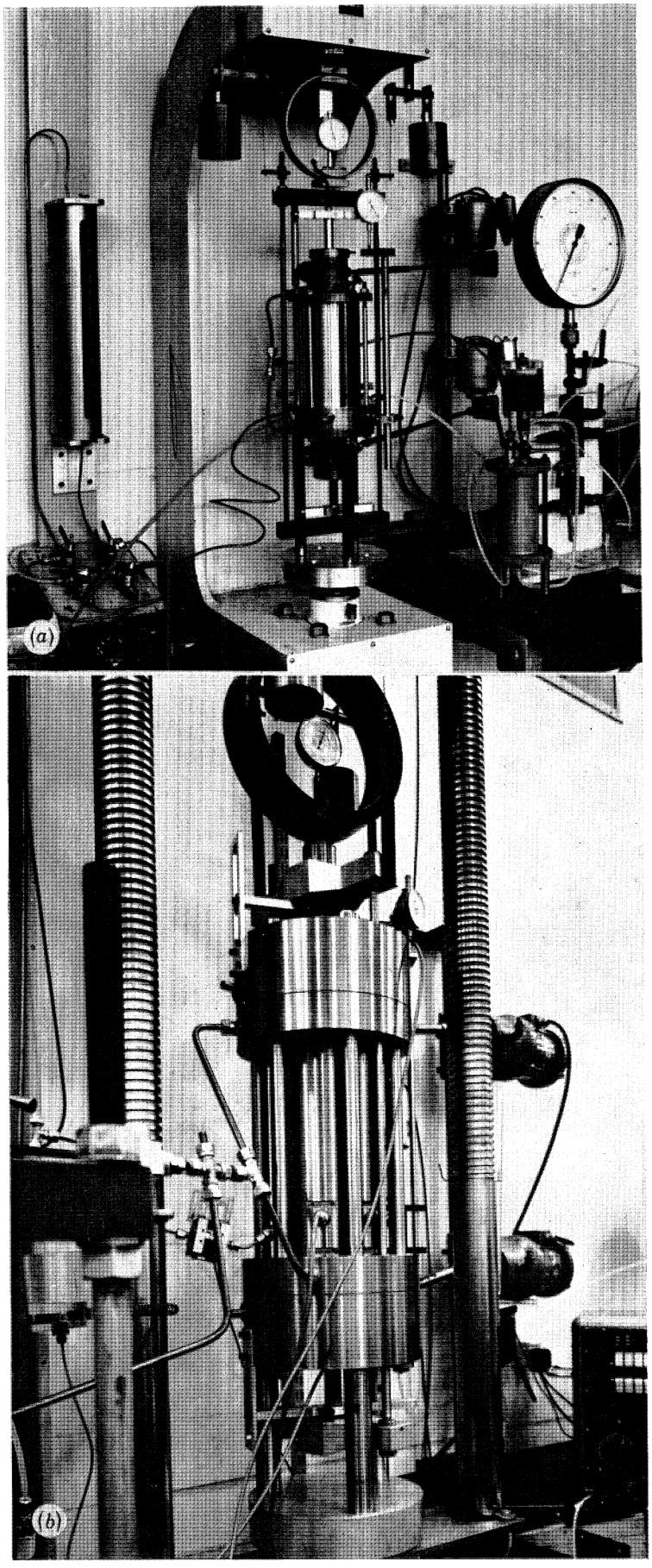

FIGURE 6. (*a*) 6.90 MN m^{-2} triaxial apparatus. (*b*) 68.95 MN m^{-2} triaxial cell.

(*Facing p.* 100)

PHILOSOPHICAL TRANSACTIONS OF THE ROYAL SOCIETY A MATHEMATICAL, PHYSICAL & ENGINEERING SCIENCES

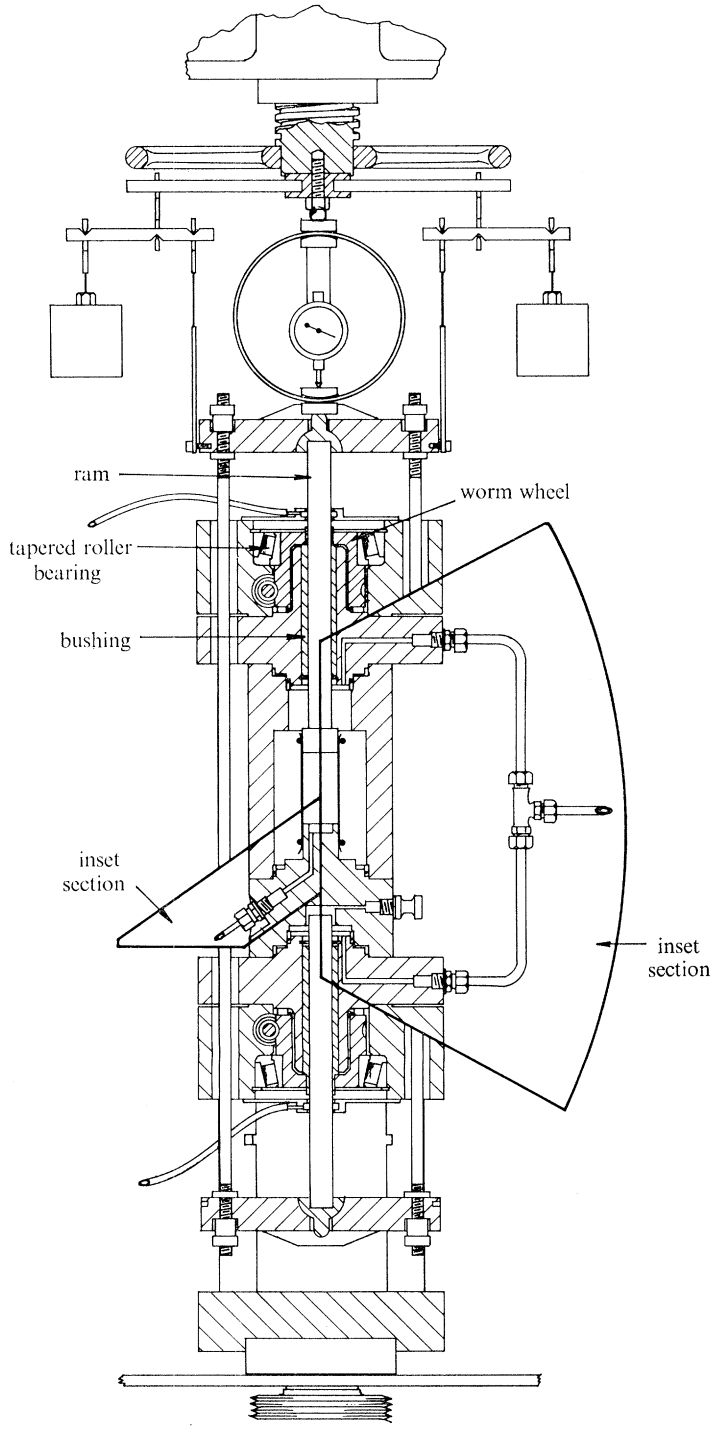

FIGURE 7. Triaxial cell with hydraulically balanced rams suitable for sample confining pressures up to 69 MN m^{-2}.

PHILOSOPHICAL TRANSACTIONS OF THE ROYAL SOCIETY A MATHEMATICAL, PHYSICAL & ENGINEERING SCIENCES

Honing to these small tolerances and the avoidance of seizing were made possible by the use of a special (spheroidal) cast iron bushing in conjunction with a stainless steel ram. The internal and external drainage paths along the bushing were 165 mm (6.500 in) and 143 mm (5.625 in) respectively. The oil loss from the pair of bushings was only about 0.75 l/h using Germ Dynobear L oil (relative density 0.892 at 15.5 °C; viscosity Redwood No. 1 at 21.1 °C 342 s; light machine tool lubricant with increased oiliness characteristic which prevents stick–slip behaviour) at the maximum cell pressure of 69 MN/m² (10 000 lbf/in²).

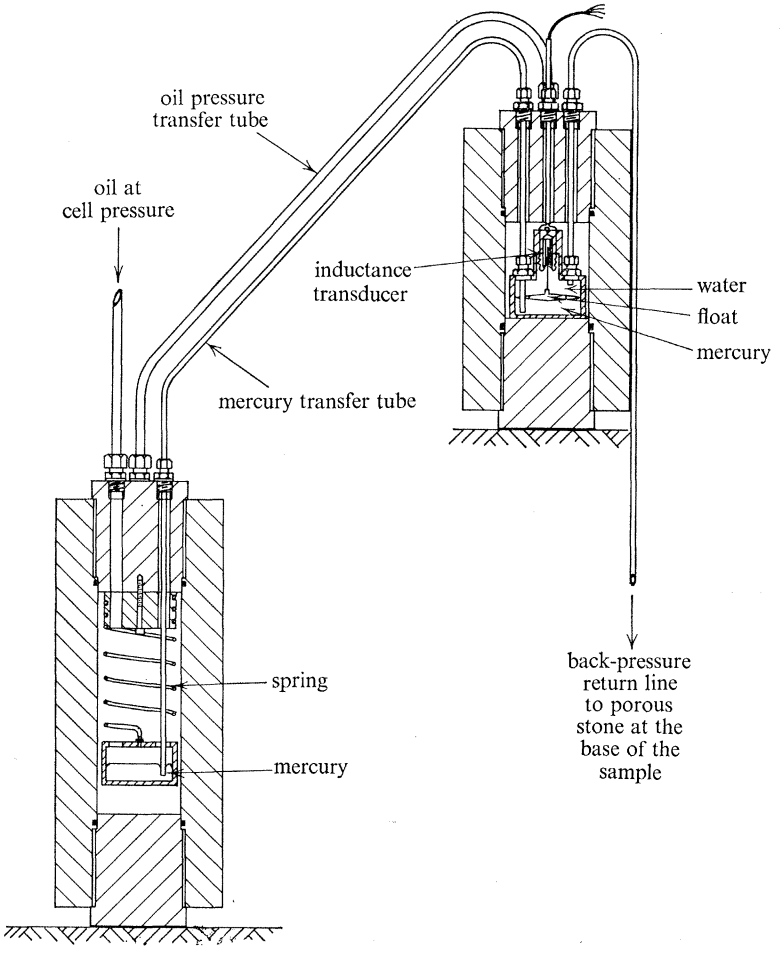

FIGURE 8. Apparatus used for $\sigma_3 - u$ = const. tests at high confining pressures, incorporating a volume gauge for tests involving high back pressures.

The second problem was the uplift force due to the cell pressure acting on the inner end of the bushing itself. Even using the minimum wall thickness convenient for manufacture and for transmitting the torque under operating conditions (6.35 mm or 0.25 in), the axial load at maximum cell pressure is 43.6 KN (9812 lbf). This load had to be carried by a thrust bearing with the minimum of vibration and friction. A tapered roller bearing (figure 7) was used for this purpose and was mounted on the boss of the bronze worm wheel which served to transmit both the torque to the rotating bush and the axial load from the bush to the inner race of the bearing. The friction between the bush and the worm wheel due to the axial load was sufficient to carry the torque necessary under most operating conditions without any form of key.

The third problem was the distortion of the loading head itself, due to the high cell pressure, which could result in unacceptable changes in diameter of the bore within which the bushing had to run. Because of the difficulty of determining these changes in bore diameter analytically, a model of the head was made in brass, strain gauged and tested. As a result of these observations the loading head was redesigned so that the major thrust on the head passed directly across to the clamping rings via the cell wall or pedestal base (figure 7).

The success of the mechanical system and the accuracy of the workmanship involved is indicated by the observation that the difference in axial load for a change in confining pressure of 69 MN/m² (10 000 lbf/in²) was less than 0.27 N (0.06 lbf).

One other aspect of the apparatus is of special interest. In the main series of tests the difference between the cell pressure and the pore-water pressure $(\sigma_3 - u)$ had to be maintained very accurately at a constant value while the cell pressure and pore-water pressure were varied through a range some 100 times the magnitude of $(\sigma - u)$. This was achieved by building a system equivalent to the constant pressure self-compensating mercury control system described by Bishop & Henkel (1962) and immersing it in fluid at the operating pressure of the cell, contained in two pressure vessels separated by an appropriate vertical distance (figure 8).

As in the widely used low pressure version, the difference between the pressure (σ_3) in the fluid above the mercury surface in the suspended cylinder in the lower vessel and in the return line (u) from the fluid above the mercury in the fixed cylinder in the upper vessel is the difference in level multiplied by the difference in the unit weights of mercury and the operating fluid in the return line R (figure 9). As the return line is connected to the porous element at the base of the sample, the change in the mercury level in the upper cylinder provides a measure of the volume change in the test specimen. This measurement is based on the volume of pore water moving in or out of the specimen and is subject to corrections for membrane penetration when $(\sigma_3 - u)$ is changed, and for the compressibility of the pore water in the sample, of the soil particles, of the water in the cell base and return line and for the expansion of the thick-walled tubing when u is changed with $(\sigma_3 - u)$ held constant.

The mercury level was sensed with an inductance transducer, the core of which was attached to a flat conical stainless steel float (figure 8). The capacity of the system as a volume gauge was 20 cm³. The overall discrimination of the system was 1×10^{-4} cm³, but the repeatability was only of the order of ± 0.01 cm³. As the initial volume of the specimens was of the order of 90 cm³ this degree of accuracy was adequate for studying the shear strength and dilatancy characteristics of the soil as a granular mass, but not for investigating in detail the influence of grain compressibility on overall volume change.

The change in the pre-set value of $\sigma_3 - u$, which would result from a change in the mercury levels consequent on a volume change in the sample, is automatically compensated for by the calibrated spring in the lower pressure vessel. As the weight of mercury in the cylinder suspended from this spring changes due to the change in mercury level in the upper cylinder a spring of suitable characteristics adjusts the lower mercury level to maintain constant pressure to an accuracy of better than ± 1 kN/m² (*ca.* ± 0.1 lbf/in²).

The high pressure cell is illustrated in figure 6*b*, plate 1.

The test programme itself was in principle very simple and consisted of the observation of the strength changes resulting from large changes in σ_3 and u, the difference $(\sigma_3 - u)$ being held constant to a high degree of accuracy. Since the natural scatter of a series of separate tests on individual samples might mask small strength changes, advantage was taken of the relatively

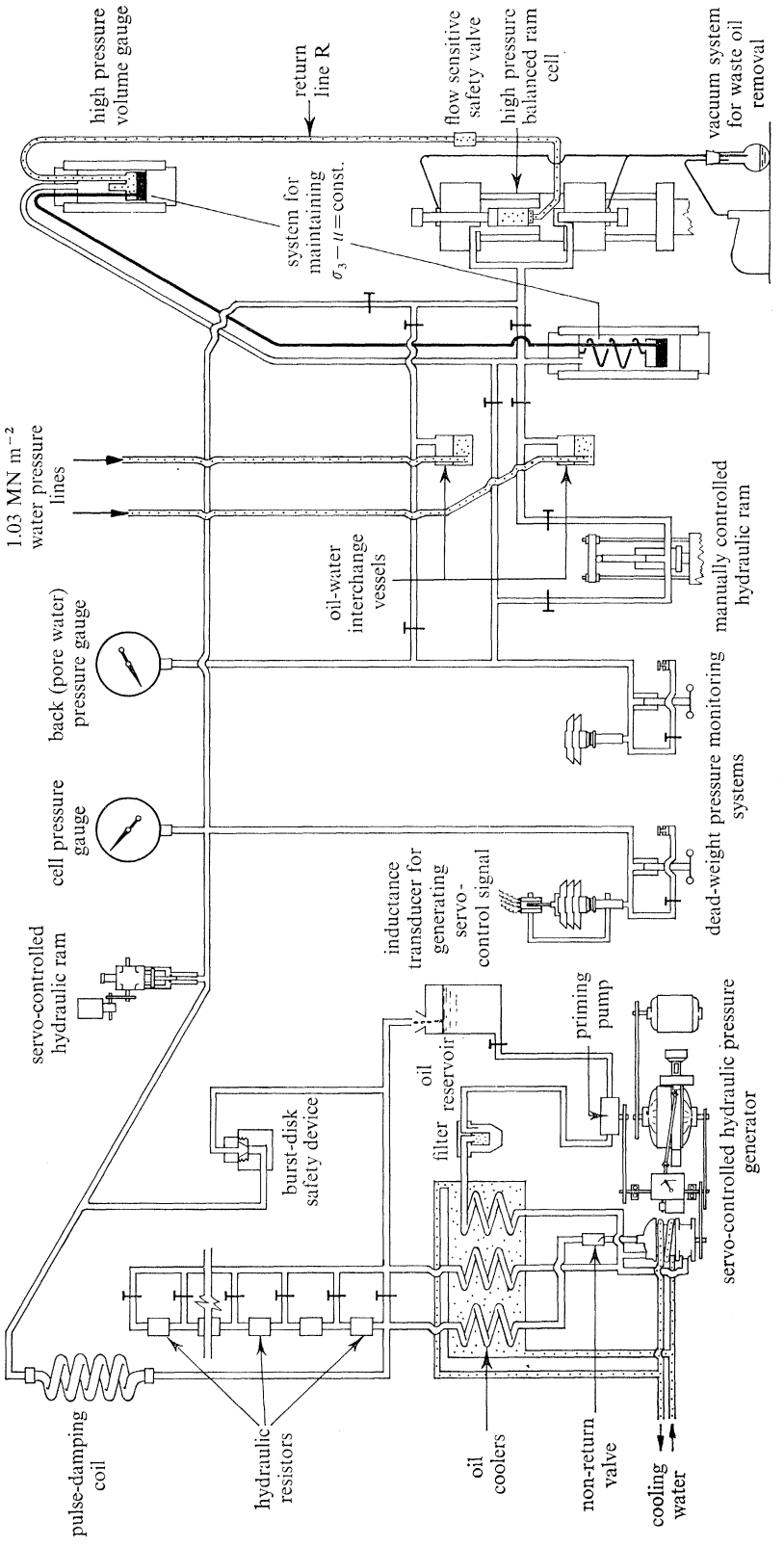

FIGURE 9. Diagrammatic layout of triaxial apparatus used for tests with cell pressures up to 69 MN m^{-2}.

small rate of change of mobilized strength with strain in loose granular materials to perform multistage tests on a limited number of specimens. If the *au* term were found to have an effect on strength, this could then be detected with an accuracy of about $\pm 0.5\,\%$ from the discontinuities in the stress–strain curve (as indicated diagrammatically in figure 10).

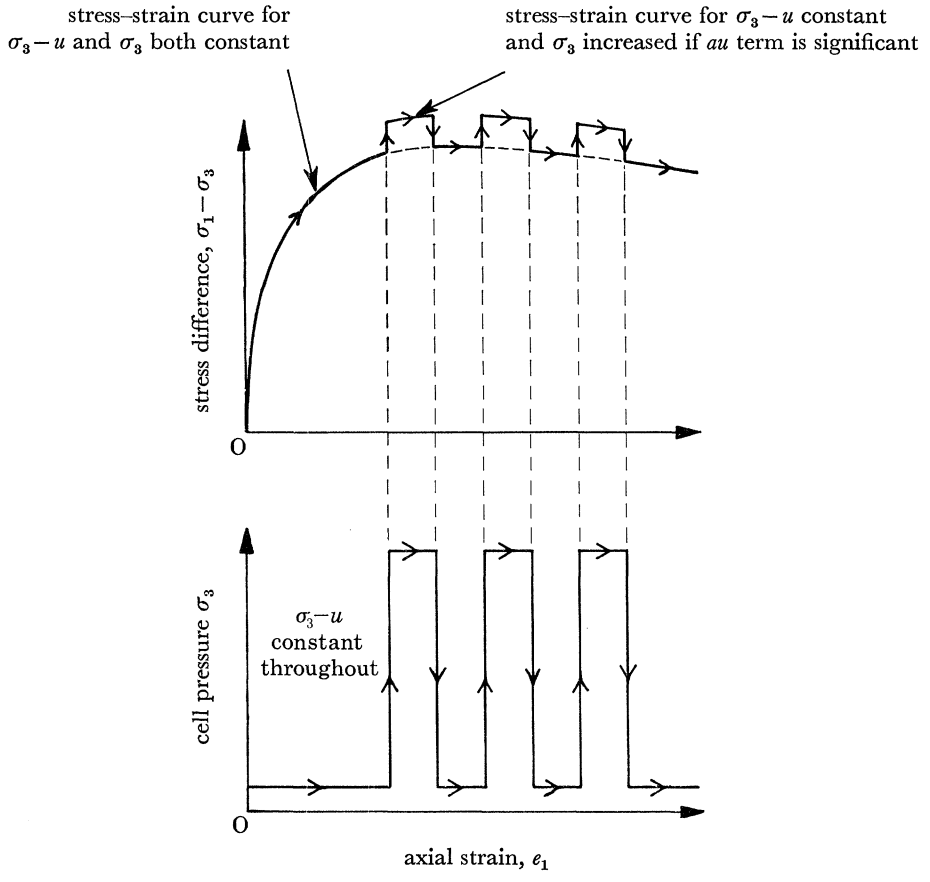

FIGURE 10. Effect on shearing resistance, in a drained triaxial compression test with σ_3-u constant, of the same large change in both confining pressure σ_3 and pore pressure u if the term *au* is significant.

All tests were performed on saturated material and the samples were sedimented under water within a rubber membrane enclosed by a split former as described by Bishop & Henkel (1962). After the sample cap had been placed in position and the membrane sealed to it a small negative pressure was applied to the pore water. This consolidated the sample by drainage through the porous ceramic disk set in the pedestal, and gave it sufficient strength for the former to be removed and the initial dimensions measured. The remaining components of the cell were then assembled and the balance of the pressure difference (σ_3-u) applied, the volume change being measured as described above.

During the application of the stress difference $(\sigma_1-\sigma_3)$ the tests were run as controlled rate of strain drained tests with constant (σ_3-u), the axial load, axial displacement and volume change being recorded. The test procedure in general follows Bishop & Henkel (1962) and is described in detail by Skinner (1975).

4. Materials tested

Four materials were tested and their particle size distribution curves are given in figure 11. They are

(1) *Ham River sand.* This is a sieved fraction of a naturally occurring gravel and is composed largely of quartz. The detailed mineral composition is given in table 2.

Ham River sand was selected as its mechanical properties have been extensively studied both at Imperial College and at the Building Research Establishment over the past 25 years in relation to strength and deformation, and to the performance of model foundations.

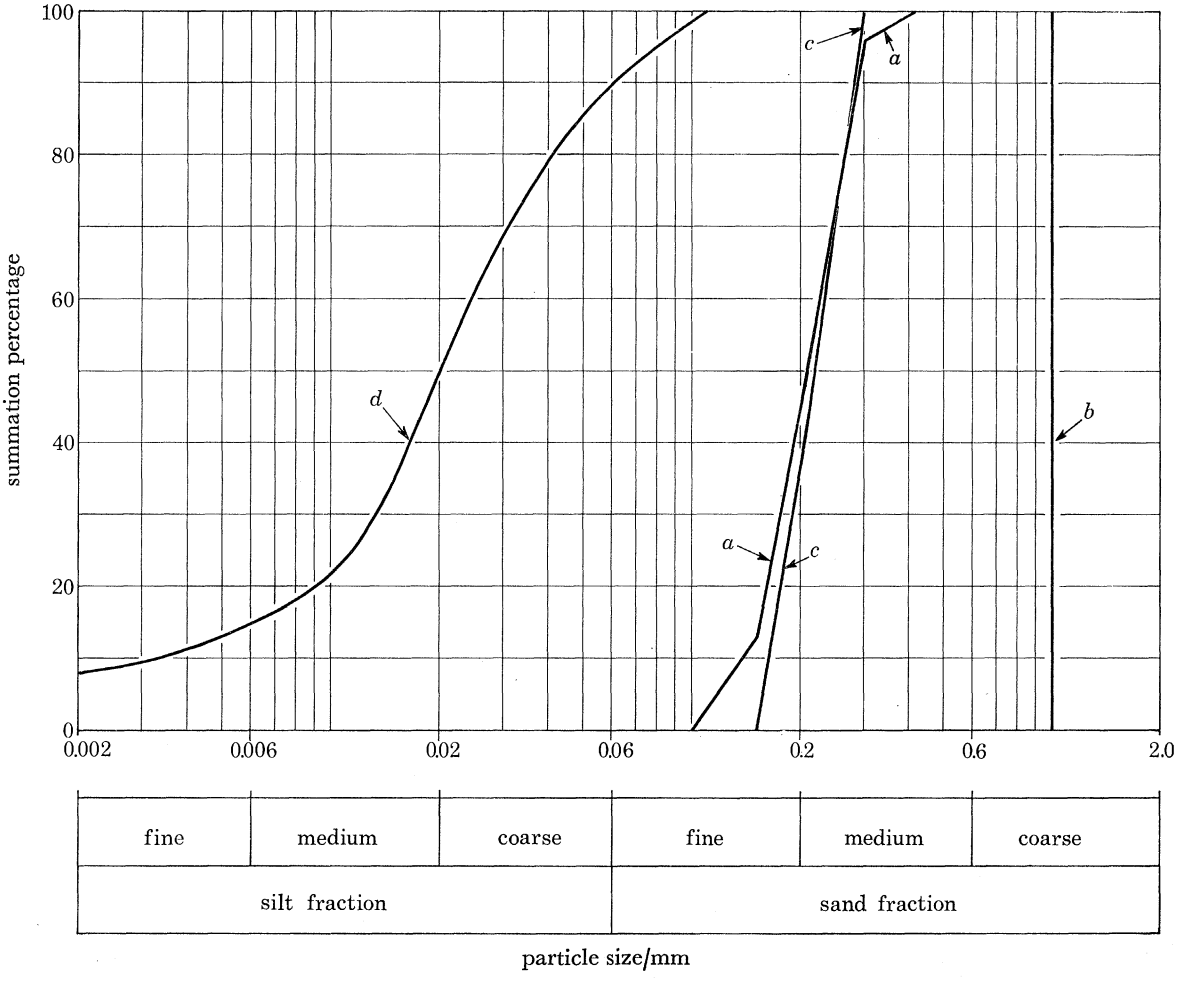

Figure 11. Particle size distribution curves for (*a*) Ham river sand; (*b*) lead shot; (*c*) crushed marble and (*d*) Braehead silt.

(2) *Lead shot.* This material had a uniform particle size of 1 mm, and was selected as a convenient and readily available material with a very low yield stress. The interparticle contact area was thus almost the maximum obtainable for a given stress level, in contrast to that of quartz sand, which is almost the minimum.

(3) *Crushed marble.* Since lead shot has a very low value of the intrinsic angle of friction ψ (*ca.* $\frac{3}{4}°$), its behaviour does not provide a very critical test of Skempton's effective stress equation

(equation (5)), since even when the product au is large for a given stress level, the factor $\tan\psi/\tan\phi'$ is very small. Calcite has the advantage of a relatively low yield stress k associated with a value of ψ of 8° (i.e. about one half of that of quartz) and can therefore provide more critical test data.

(4) *Braehead silt.* This material is a naturally occurring silt, composed mainly of quartz, but having an average particle size more than an order of magnitude smaller than the Ham River sand. The detailed mineral composition is given in table 2. Since the force per contact, for a given geometrical arrangement of particles, is proportional to d^2, where d is the equivalent diameter of the particle, this force is likely to be at least two orders of magnitude smaller for the silt than for the Ham River sand. Furthermore, about 7 % of the particles are smaller than 2 μm and the material has a significant plasticity index (6 %). It might be expected to indicate the beginning of any trend in behaviour as the grading moves towards that of materials classified as clays.

TABLE 2

mineral composition of Ham River sand		mineral composition of Braehead silt	
quartz	96.22 %	quartz	95.20 %
limonite	3.66 %	illite	2.80 %
zircon	0.10 %	kaolinite	1.60 %
staurolite	0.02 %	chlorite	0.40 %

analysis by Midgley (Building Research Station)

The time scale of fully drained tests on clay is so very much longer (involving weeks rather than hours) that a different pressure control and data logging system is required. Clays were therefore not included in the present programme.

5. TEST RESULTS AND THEIR IMPLICATIONS

The most extensive series of tests was run on the Ham River sand, involving substantial variations in the value of $(\sigma - u)$ as well as in the coupled values of σ and u. Individual tests were then run on each of the selected materials.

(a) *Ham River sand*

Two tests run in the prototype apparatus with $(\sigma_3 - u)$ equal to 69.0 kN/m² (10.0 lbf/in²) and a variation of σ_3 between 345 kN/m² (50 lbf/in²) and 6.9 MN/m² (1000 lbf/in²) are illustrated in figures 12 and 13. It is immediately apparent that for a change in the value of u of 6.55 MN/m² (950 lbf/in²) there is no discernible change in shearing resistance resulting from a change in pore pressure with $(\sigma_3 - u)$ held constant.

The results of three tests run in the high pressure apparatus with $(\sigma_3 - u)$ equal to 363 kN/m² (52.6 lbf/in²) and a variation of σ_3 between 1.03 MN/m² (150 lbf/in²) and 27.58 MN/m² (4000 lbf/in²) are shown in figures 14, 15 and 16. Substantially the same conclusion can be drawn as before, although slight irregularities are observed while the changes in σ_3 and u are actually being made. This is attributed to small pressure gradients resulting from the flow of the relatively compressible pore fluid under the large pressure changes, in particular in the small bore high pressure lines connecting the pressure vessels maintaining value of u at a constant difference from σ_3.

These three tests are of particular interest since the value of $(\sigma_3 - u)$ is typical of the range encountered in engineering practice and the change in u of 26.5 MN/m² (3850 lbf/in²) exceeds this value by a factor of 73 times. Had the value of the contact area a equalled the maximum value

PHILOSOPHICAL TRANSACTIONS OF THE ROYAL SOCIETY A MATHEMATICAL, PHYSICAL & ENGINEERING SCIENCES

envisaged for sand by Bishop & Eldin (1950), its value on the relevant shear surface in the present tests would have been *ca.* 0.4 %. The value of the term Δr (equal to $a\Delta u/(\sigma_n - u)$)† would have been of the order 0.004×46.8 i.e. 0.19. Both of the theories involving an au term would thus have predicted substantial discontinuities in the stress–strain curve when the value of u was varied with $\sigma_3 - u$ constant.

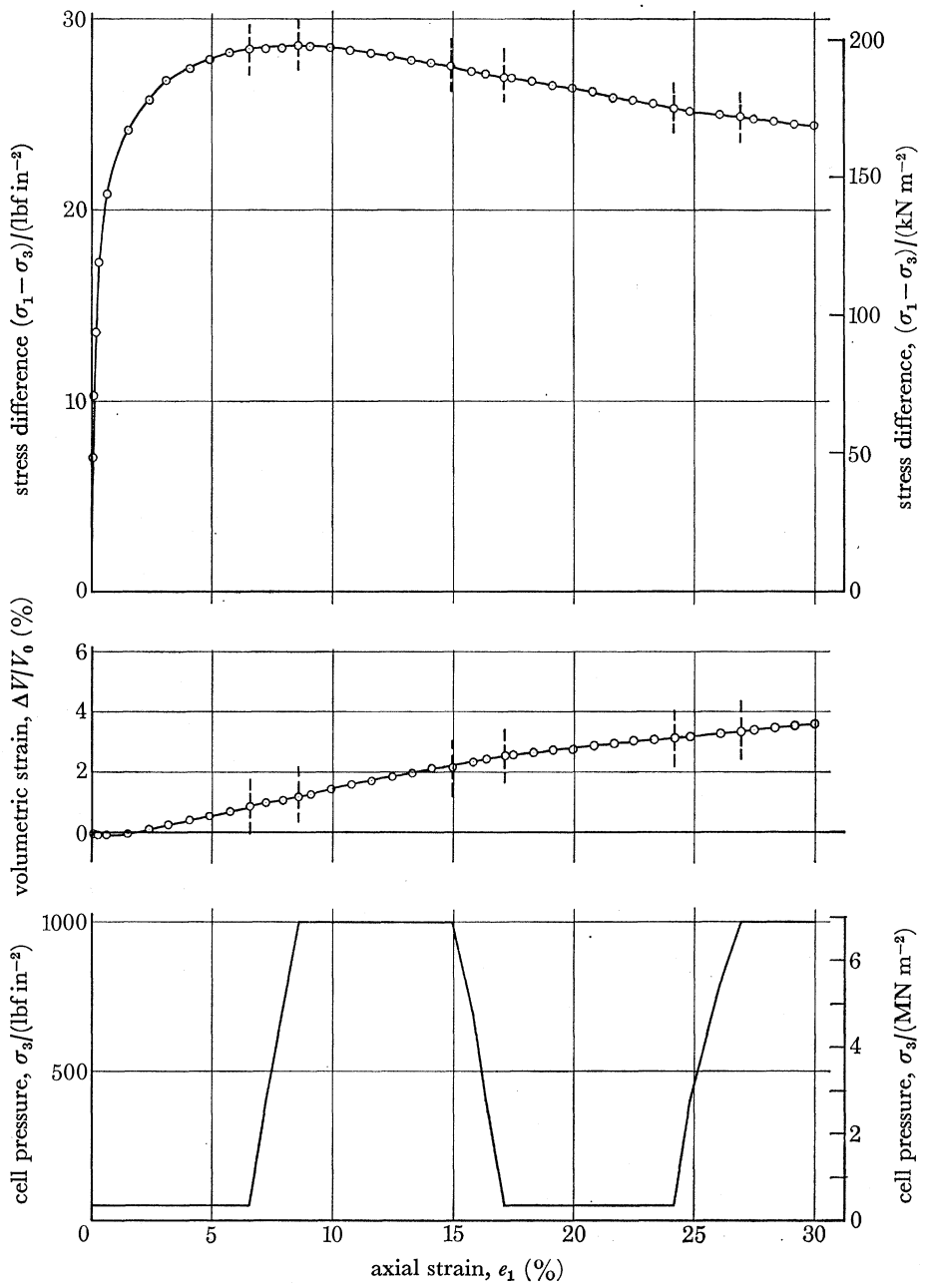

FIGURE 12. Ham river sand tested with $(\sigma_3 - u)$ = 69.0 kN m^{-2} (10 lbf in^{-2}) (sample porosity at the start of the shear stage = 43.4 %).

† In any state of stress other than that of isotropic stress the value of a in a particulate material and the value of the ratio $\Delta u/(\sigma - u)$ will have directional properties. Skempton (1960) has presented his analysis in terms of the Mohr–Coulomb failure criterion, in which the normal effective stress on the shear surface (*ca.* $(\sigma_n - u)$) is $(1 + \sin\phi')$ times the minor effective stress (*ca.* $(\sigma_3 - u)$). This point is discussed in more detail in subsequent paragraphs.

It is therefore pertinent to re-examine the possible range of values of the contact area a, in particular in the light of the micro-indentation hardness data published, for example, by Brace (1963).

Bishop & Eldin (1950) related σ_p, the value of the average interparticle contact pressure, to S, the value of the crushing strength of the grains, by the expression

$$\sigma_p - u = bS, \tag{10}$$

where the constant b will depend on the type of surface failure produced, but with a minimum value probably not much lower than unity.

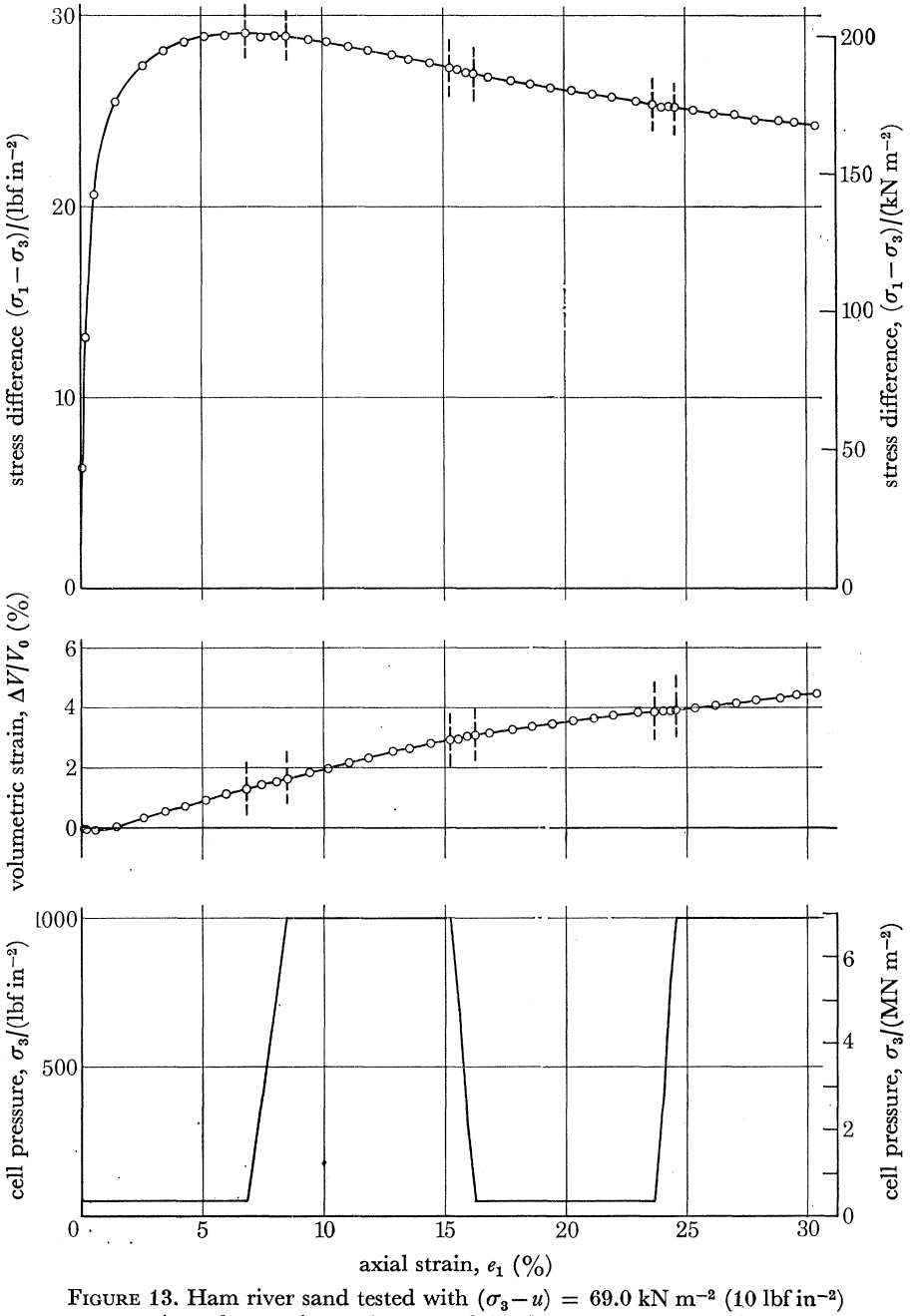

FIGURE 13. Ham river sand tested with (σ_3-u) = 69.0 kN m^{-2} (10 lbf in^{-2}) (sample porosity at the start of the shear stage = 40.9 %).

The intergranular stress σ_i (defined as the intergranular force per unit area) was related to σ_p by the expression

$$\sigma_i = a\sigma_p. \tag{11}$$

Since σ_i is related to σ and u by equation (2):

$$\sigma_i = (\sigma - u) + au,$$

we have, from equations (10) and (11),

$$(\sigma - u) + au = abS + au$$

or

$$a = \frac{\sigma - u}{bS}. \tag{12}$$

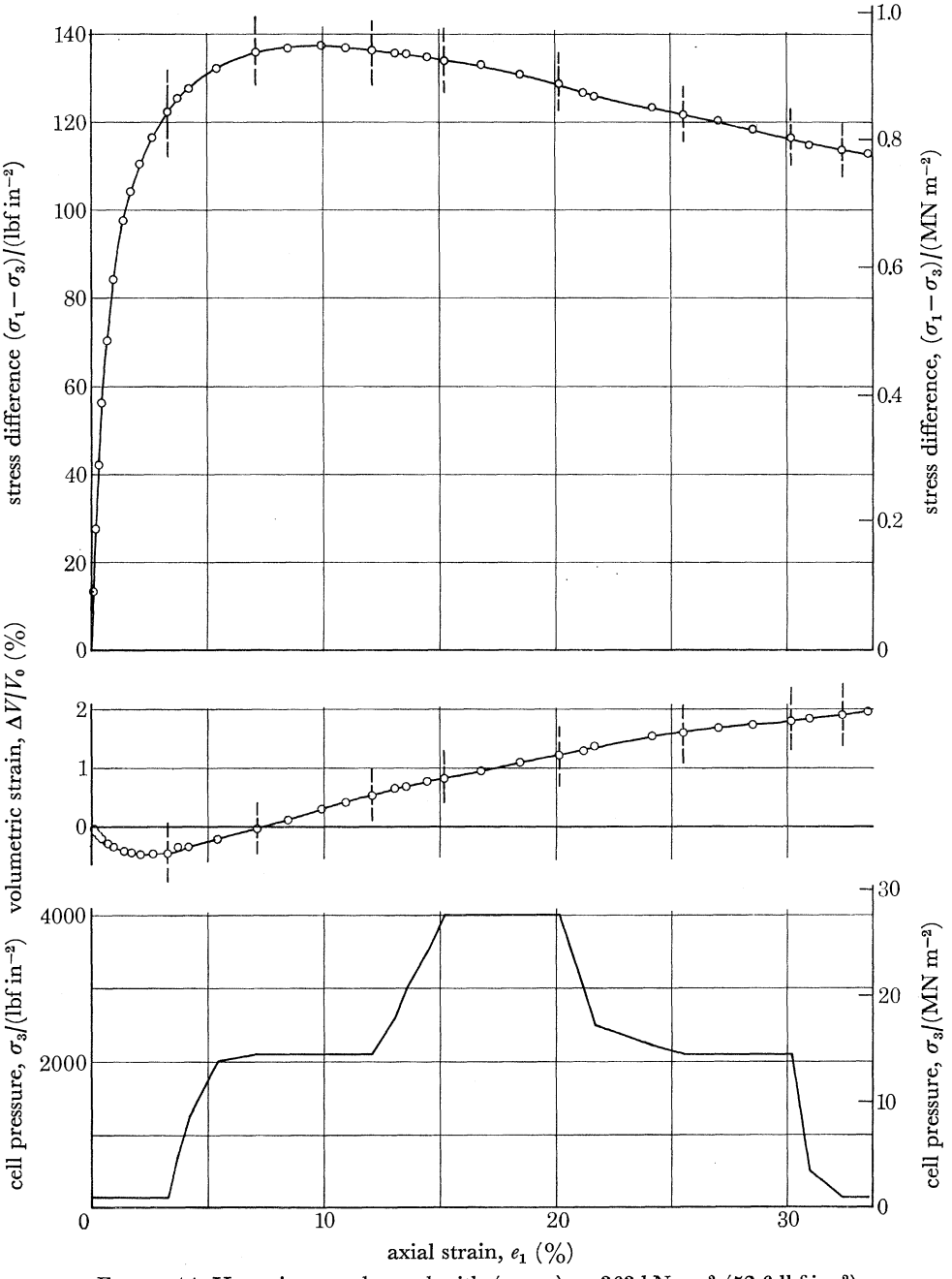

FIGURE 14. Ham river sand tested with $(\sigma_3 - u) = 363$ kN m^{-2} (52.6 lbf in^{-2}).

Skempton (1960) gives an expression for the general case of a cohesive particulate material with an initial contact area a_0 at zero stress, with the assumption that junction growth during shear is negligible:

$$a - a_0 = \frac{\sigma - u}{Mk}, \tag{13}$$

where k is the intrinsic cohesion defined in equation (4) and

$$M = \frac{2\cos\psi}{1-\sin\psi}.$$

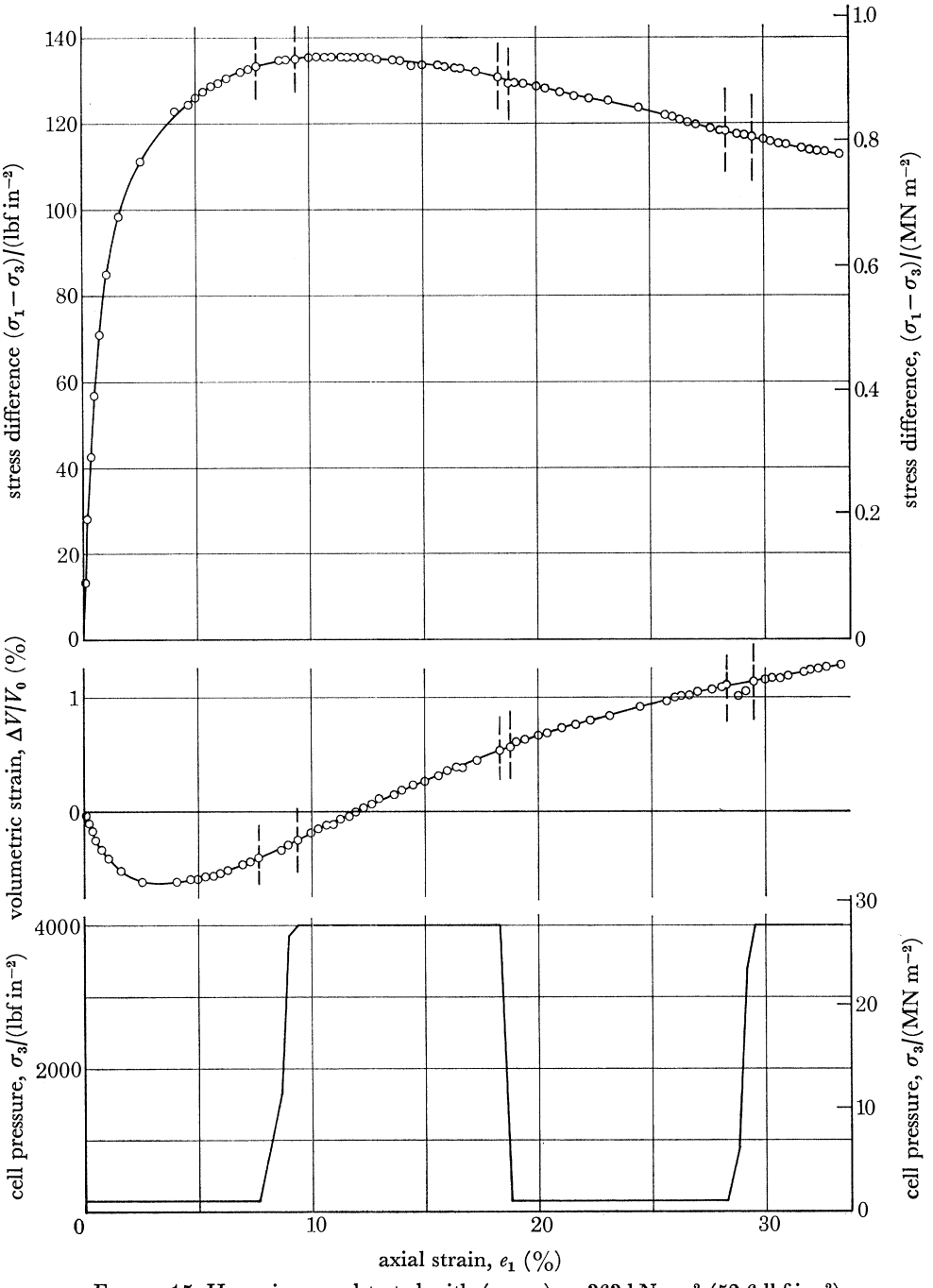

FIGURE 15. Ham river sand tested with $(\sigma_3 - u) = 363$ kN m^{-2} (52.6 lbf in^{-2}).

Since it follows from the geometry of the Mohr diagram (figure 17) that,

$$\sigma_1 - \sigma_3 = k\frac{2\cos\psi}{1-\sin\psi} + \sigma_3\frac{2\sin\psi}{1-\sin\psi}, \tag{14}$$

then S, which is equal to $\sigma_1 - \sigma_3$ when σ_3 is zero, is given by the expression

$$S = k\frac{2\cos\psi}{1-\sin\psi}, \tag{15}$$

i.e.

$$S = Mk. \tag{16}$$

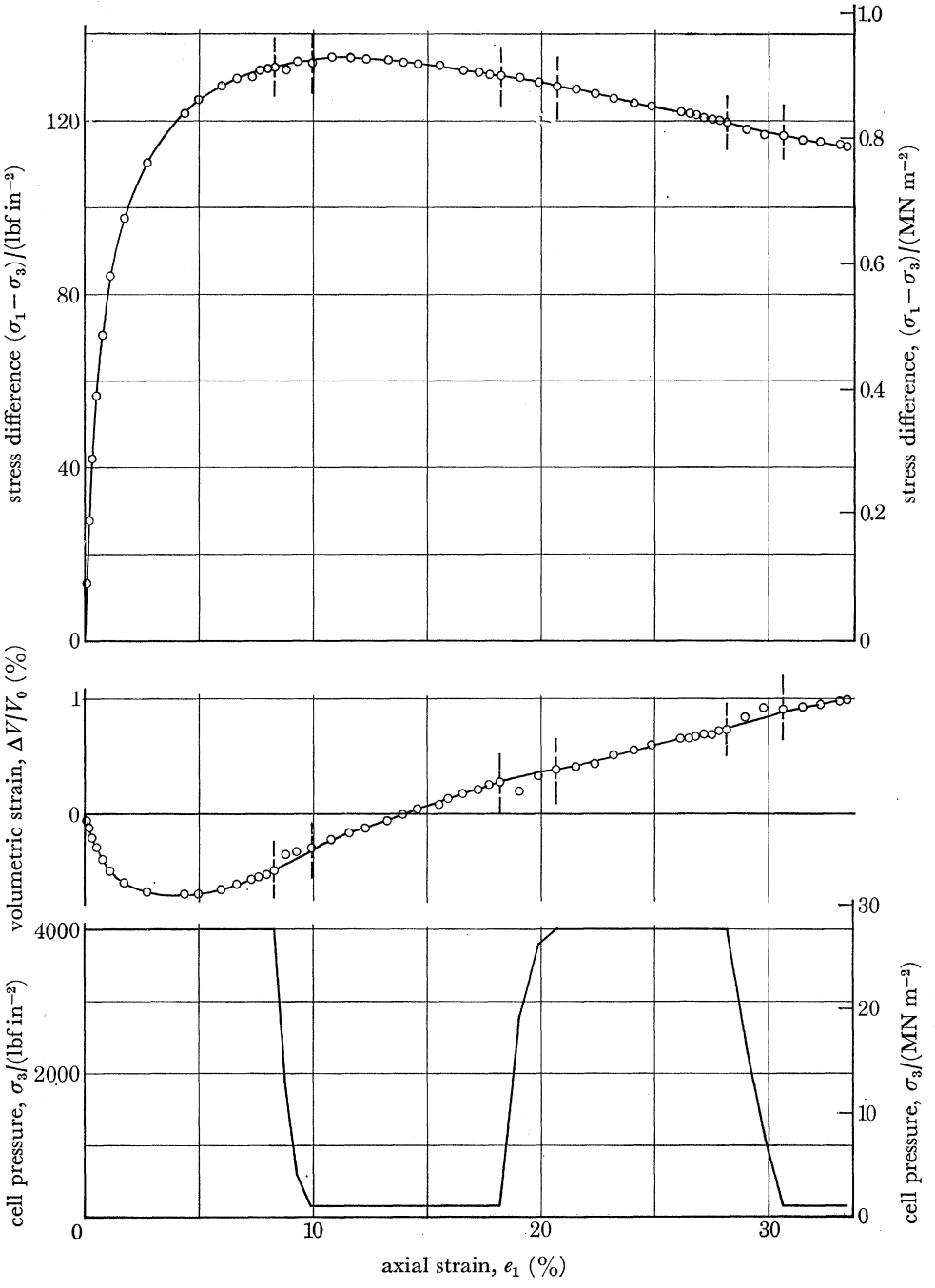

FIGURE 16. Ham river sand tested with $(\sigma_3 - u)$ = 363 kN m^{-2} (52.6 lbf in^{-2}).

For a sand recently sedimented in water (as in the present case) a_0 may be taken as zero. Equations (12) and (13) then give the same value of contact area a if the coefficient b in equation (12) is assumed to be equal to unity.†

Taking the values of k and ψ for intact quartz from Skempton (1960), 932 MN/m² (9500 kgf/cm²) and $13\frac{1}{4}°$ respectively, we have from equation (15) a value of S equal to 2255 MN/m². This is more than an order of magnitude greater than the value of 138 MN/m² used by Bishop & Eldin (1950) on the basis of the strength of granites and quartzites under low hydrostatic pressures. The calculated contact area on the shear surface corresponding to the state of stress in the tests run with $(\sigma_3 - u) = 363$ kN/m² drops from 0.4 % to *ca.* 0.025 %.

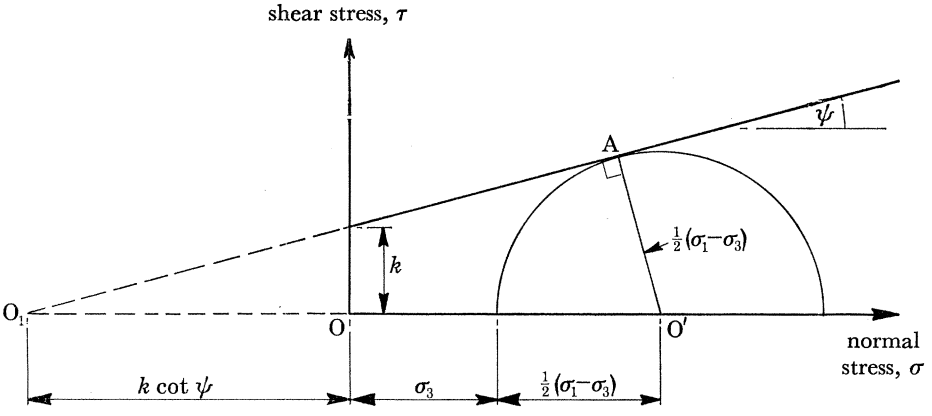

$$\sin\psi = \frac{AO'}{O_1O'}, \text{ hence } (\sigma_1 - \sigma_3) = k\,\frac{2\cos\psi}{1-\sin\psi} + \sigma_3\,\frac{2\sin\psi}{1-\sin\psi}$$

FIGURE 17. The geometry of the Mohr diagram for a solid with intrinsic cohesion and friction.

Even with this lower value of a the value of $a\Delta u/(\sigma_n - u)$ is 0.012. This would imply discontinuities of 1.2 % in the resistance to shear as the value of u was varied between the upper and lower limits if the intergranular stress controlled the shear strength. These would have been clearly discernible. In the case of Skempton's effective stress equation the factor $\tan\psi/\tan\phi'$ reduces the implied percentage discontinuity to 0.4 % (for $\psi = 13\frac{1}{4}°$ and $\phi' = 34.2°$ as in the test illustrated in figure 15.)This value is at the limit of discrimination of the test. On this basis, and for pore pressure changes of this magnitude, it is apparent that the predictions of the Terzaghi effective stress equation and Skempton's effective stress equation do not differ significantly from each other or from the observed behaviour of quartz sand in a multistage test.

However, the prediction of the value of a, which forms the basis both of the intergranular stress equation and of Skempton's equation, has so far been made without attempting to evaluate the influence either of junction growth or of the actual magnitude of the interparticle contact forces. Before examining these two factors it is necessary to look more closely at the conditions under which the Mohr–Coulomb failure criterion can be used to relate the shear strength τ_f on a plane on which the normal effective stress is σ_n' (to which Skempton's analysis applies) to the principal stresses in an axially symmetrical compression test (as used in the present experimental program).

† There is evidence that b may rise to about 3 for metals (Bowden & Tabor 1950). The predicted contact area would be correspondingly reduced, a point which is discussed further in relation to the tests on lead shot where there is direct evidence of the magnitude of the area of contact.

In the absence of pore pressure the effective stresses equal the total stresses and the Mohr–Coulomb criterion is given by the expression

$$\tau_f = c + \sigma \tan \phi. \tag{17}$$

The theory can be applied rigorously only if the parameters c and ϕ are invariant with respect to changes in the inclination θ of the reference plane (figure 18), changes in the stresses on this plane being given by the expressions:

$$\tau = \tfrac{1}{2}(\sigma_1 - \sigma_3) \sin 2\theta, \tag{18}$$

$$\sigma_n = \tfrac{1}{2}(\sigma_1 + \sigma_3) + \tfrac{1}{2}(\sigma_1 - \sigma_3) \cos 2\theta, \tag{19}$$

where σ_1 and σ_3 denote the major and minor principal stresses.

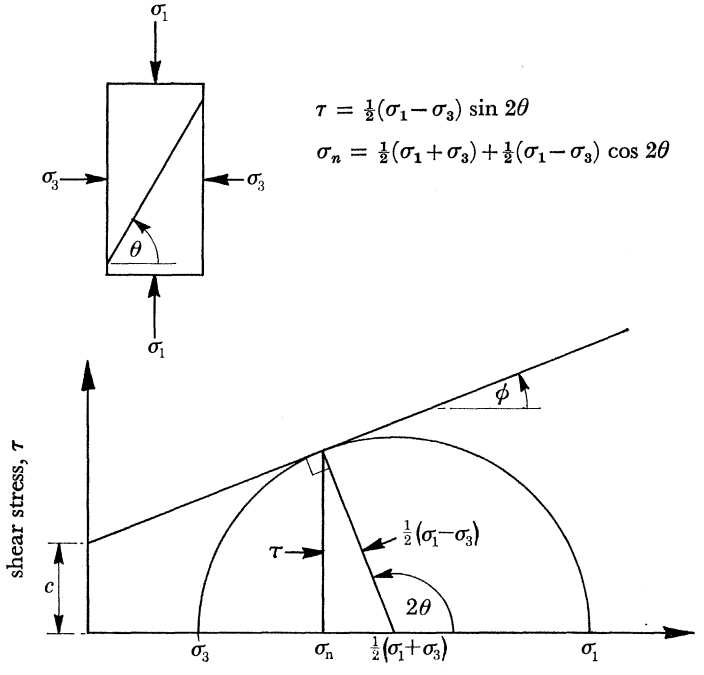

FIGURE 18. Stresses on the reference plane.

It follows from the conventional analysis for isotropic materials that the shear surface is inclined at an angle θ, where $\theta = 45° + \frac{1}{2}\phi'$, and that the principal stress difference is related to the minor principal stress by the expression

$$(\sigma_1 - \sigma_3)_f = c \frac{2 \cos \phi}{1 - \sin \phi} + \sigma_3 \frac{2 \sin \phi}{1 - \sin \phi}. \tag{20}$$

This application of the Mohr–Coulomb failure criterion to effective stresses presents no difficulty if the Terzaghi expression $\sigma' = \sigma - u$ is used, since u is invariant with respect to changes in the inclination θ of the reference plane. However, in terms of intergranular stress, we have the expression

$$\tau_f = c' + \{(\sigma - u) + au\} \tan \phi'. \tag{21}$$

Skempton's expression for effective stress gives

$$\tau_f = c' + \left\{(\sigma - u) + au \frac{\tan \psi}{\tan \phi'}\right\} \tan \phi'. \tag{22}$$

In both cases a is *not* invariant with respect to changes in θ. The expression for a (without junction growth) given in equation (13) is

$$a = a_0 + \frac{\sigma - u}{Mk}.$$

Substituting in equation (22) we have

$$\tau_f = c' + \left\{(\sigma - u) + u\left(a_0 + \frac{\sigma - u}{Mk}\right)\frac{\tan\psi}{\tan\phi'}\right\}\tan\phi'.$$

Assuming a_0 to be an isotropic property, and collecting the terms which vary with σ we obtain:

$$\tau_f = c' + ua_0\frac{\tan\psi}{\tan\phi'}\tan\phi' + (\sigma - u)\left\{1 + \frac{u}{Mk}\frac{\tan\psi}{\tan\phi'}\right\}\tan\phi'. \tag{23}$$

In terms of the Mohr–Coulomb failure criterion we now have a new material in which the parameters c' and ϕ' are replaced by $(c')_u$ and $(\phi')_u$ where

$$(c')_u = c' + u\left(a_0\frac{\tan\psi}{\tan\phi'}\right)\tan\phi', \tag{24}$$

and

$$(\phi')_u = \arctan\left\{\left(1 + \frac{u}{Mk}\frac{\tan\psi}{\tan\phi'}\right)\tan\phi'\right\}. \tag{25}$$

The term $(\sigma - u)$ then correctly reflects the variation in normal stress with change in the value of θ, since u is invariant for each particular stage of a multistage test.

We may therefore replace c and ϕ in equation (20) by the expressions given in equations (24) and (25) and replace σ_3 by $(\sigma_3 - u)$. For small differences between the parameters $(c')_u$ and c', and $(\phi')_u$ and ϕ', we may obtain the change in the stress difference at failure $(\sigma_1 - \sigma_3)_f$ with a change in u by differentiating this expression with respect to u†, $(\sigma_3 - u)$ being constant as in the tests. This leads to the expression

$$\frac{\mathrm{d}(\sigma_1 - \sigma_3)_f}{\mathrm{d}u} = a_0\frac{\tan\psi}{\tan\phi'}\frac{2\sin\phi'}{(1 - \sin\phi')} + \frac{\tan\psi}{\tan\phi'}\frac{2\sin\phi'}{(1 - \sin\phi')}\left\{\frac{1}{Mk}(c'\cos\phi' + (\sigma_3 - u)(1 + \sin\phi'))\right\}. \tag{26}$$

Now it follows from the geometry of the Mohr diagram that the component of $(\sigma - u)$ normal to the shear surface is given by the expression

$$(\sigma_n - u) = c'\cos\phi' + (\sigma_3 - u)(1 + \sin\phi'). \tag{27}$$

The component of area of contact which is a function of normal stress is given by the equation

$$a_f = \frac{(\sigma_n - u)}{Mk}. \tag{28}$$

Thus the expression for the change in strength with change in pore pressure, $(\sigma_3 - u)$ being held constant, reduces to

$$\frac{\mathrm{d}(\sigma_1 - \sigma_3)_f}{\mathrm{d}u} = a_\tau\frac{\tan\psi}{\tan\phi'}\frac{2\sin\phi'}{(1 - \sin\phi')}, \tag{29}$$

where a_τ is the total contact area on the shear surface and $a_\tau = a_0 + a_f$.

This expression is the same as that arrived at by rather different reasoning by Skempton (1960). The validity of adding components of contact area may be questioned, especially in a complex

† Provided $\sin\phi'$ differs substantially from unity, a condition which is satisfied in all particulate materials.

material such as concrete, but this is not relevant to a discussion of cohesionless particulate materials in which $a_0 = 0$ and $c' = 0$. However, two other points which have to be considered are the influence of junction growth and the effect of the magnitude of the interparticle forces.

It should be noted that if the contact area ceases to be a linear function of the normal stress component $(\sigma - u)$ and varies with the magnitude of the shear stress τ, which is zero on the major and minor principal planes and a maximum when $\theta = 45°$, then the analysis presented in the preceding paragraphs is no longer strictly applicable. However, the quantification of the phenomenon of junction growth is itself subject to some uncertainty (see, for example, Bowden & Tabor 1954, 1964). It is clear that the stress path of the junction material would be of the form indicated in figure 19, and, with clean surfaces, could in the limit reach the intrinsic failure envelope of the material. Some bounds can be put to the probable values of interparticle contact pressure under normal pressure alone (σ_p) and at slip (σ_{nj}) from experimental observations of the coefficient of friction μ and the results of the micro-indentation hardness test.

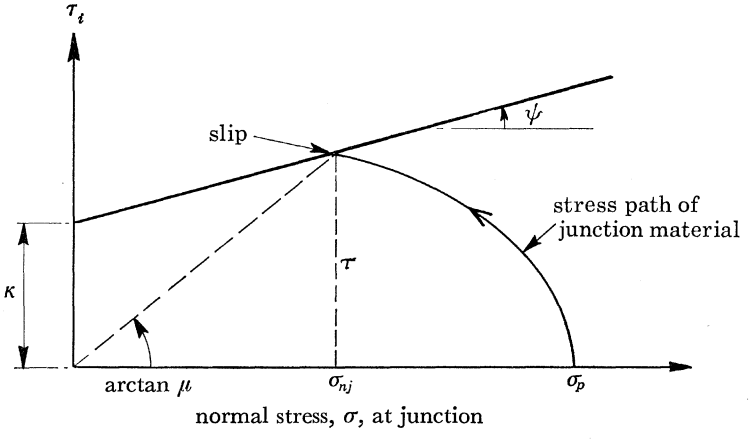

FIGURE 19

It follows from figure 19 that the lower limit of the stress σ_{nj} corresponds to the upper limit of the observed coefficient of friction. In a series of test conducted so as to ensure a clean contact between a slider and plate a value of $\mu = 0.8$ was obtained for quartz by Skinner (1975). Taking values of $\kappa = 941\,\mathrm{MN/m^2}$ and $\psi = 16\frac{1}{4}°$ for quartz (based on a re-assessment of published data), we obtain from the geometry of figure 19 a lower limit for σ_{nj} of $1851\,\mathrm{MN/m^2}$.

As a simplification we may use the expression:

$$a = \frac{(\sigma_n - u)}{\sigma_{nj}}. \tag{30}$$

This gives the maximum value of the contact area a in the test run with $(\sigma_3 - u) = 363\,\mathrm{kN/m^2}$ as

$$a = \frac{567 \times 10^{-3}}{1851}$$

$$= 3.06 \times 10^{-4},$$

the value of $(\sigma_n - u)$ being $567\,\mathrm{kN/m^2}$.

The corresponding minimum values of σ_p implicit in equation (12) (with $b = 1$) and in equation (13) are both $2510\,\mathrm{MN/m^2}$. However, depending on the geometry of the interparticle contact and on the yield pattern, the value of b may be as high as 3, leading to a value of

$\sigma_p = 7530\,\mathrm{MN/m^2}$. Without junction growth the value of a, from equation (12), would lie in the range 2.26×10^{-4} to 5.53×10^{-5}.

These values represent the largest probable values of a. The micro-indentation hardness tests on quartz published by Brace (1963), and illustrated in figure 20, suggest that at small values of the interparticle contact force the value of σ_p required to cause yield may be substantially greater than at the larger loads used on a typical slider. Based on an analysis of the stress path the corresponding value of the coefficient of friction is lower and is associated with a higher value of σ_{nl}. For an interparticle force of 2 gf (the minimum used by Brace (1963)) the value of μ drops to 0.4 and the value of σ_{nj} rises to $5688\,\mathrm{MN/m^2}$ (Skinner 1975). For the stress level under consideration the value of a (from equation (30)) drops to a value of 6.53×10^{-5}.

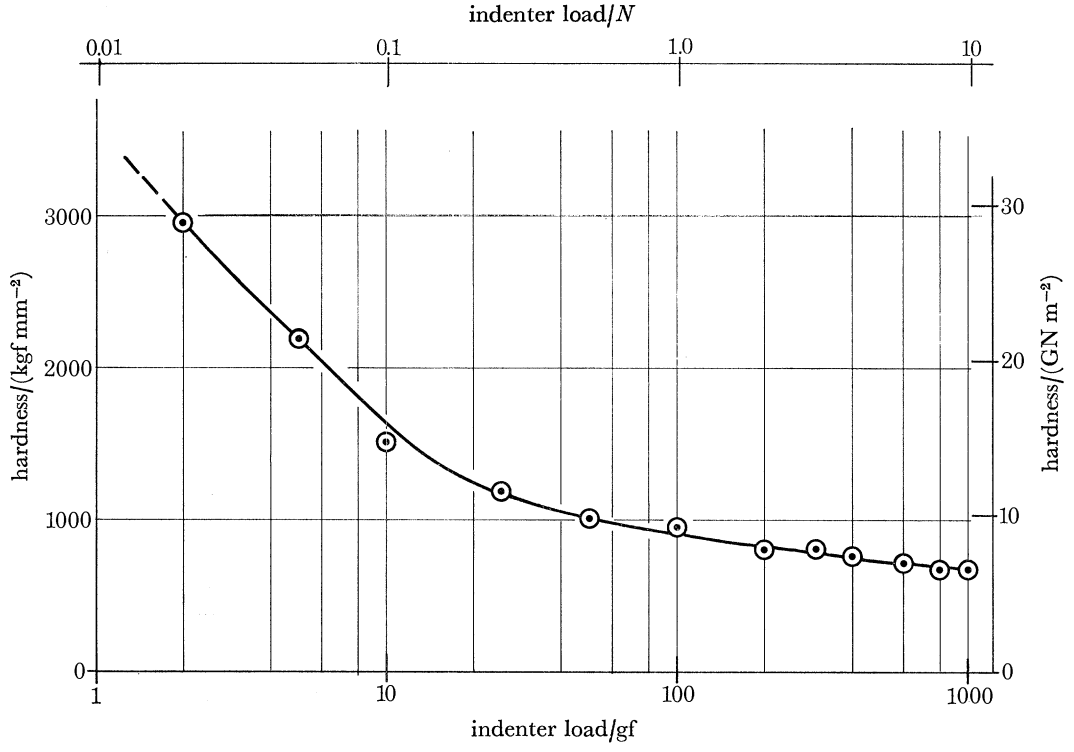

FIGURE 20. Hardness against load applied to indenter: data from Brace (1963).

It is of interest to note that for a regular cubical packing of uniform spherical particles the interparticle force P is given by the expression (Bishop 1965):

$$P = \sigma d^2. \tag{31}$$

An equivalent uniform material having the mean particle size of Ham River sand (0.2 mm diameter) and subjected to the present stress ($567\,\mathrm{kN/m^2}$) would thus have an average interparticle force P equal to 2.3 gf. This force almost certainly represents the upper limit for particles of this mean size and stress level. It may thus be inferred that the value of the contact area a tends towards the lower limit in the present tests.

The corresponding values of $\mathrm{d}(\sigma_1 - \sigma_3)_f/\mathrm{d}u$ and of the percentage change in compression strength are given in table 3, on the assumption that the error in applying equation (29) to the cases involving junction growth is acceptable in view of the other uncertainties involved. As

convincing evidence of a discontinuity in the stress–strain curve requires a jump of about 0.5 % in strength it will be seen that the interpretation to be placed on the absence of jumps depends on the significance attached to the influence of particle contact force. For a pore pressure change of this magnitude (26.5 MN/m²) the use of the Terzaghi equation is fully justified. The evidence against the intergranular stress equation is just significant, but the test is not definitive in terms of Skempton's effective stress equation.

TABLE 3. PREDICTED CHANGES IN STRENGTH FOR A CHANGE IN PORE PRESSURE $\Delta u = 26.5$ MN/m², THE VALUE OF $(\sigma_3 - u)$ BEING CONSTANT AND EQUAL TO 0.363 MN/m²

		intergranular stress equation (2)		Skempton's effective stress equation (5)		Terzaghi effective stress equation (1)	
assumption about contact area a	value of a	$\frac{\Delta(\sigma_1-\sigma_3)_f}{\text{kN/m}^2}$	$\frac{\Delta(\sigma_1-\sigma_3)_f}{(\sigma_1-\sigma_3)_f}$ (%)	$\frac{\Delta(\sigma_1-\sigma_3)_f}{\text{kN/m}^2}$	$\frac{\Delta(\sigma_1-\sigma_3)_f}{(\sigma_1-\sigma_3)_f}$ (%)	$\frac{\Delta(\sigma_1-\sigma_3)_f}{\text{kN/m}^2}$	$\frac{\Delta(\sigma_1-\sigma_3)_f}{(\sigma_1-\sigma_3)}$ (%)
without junction growth, and with $b = 1$	2.26×10^{-4}	15.4	1.65	6.61	0.71	0	0
without junction growth, and with $b = 3$	5.53×10^{-5}	3.78	0.41	1.62	0.18	0	0
with junction growth, max. probable value	3.06×10^{-4}	20.9	2.24	8.97	0.96	0	0
with junction growth, value corresponding to load of 2 gf per contact	6.53×10^{-5}	4.46	0.48	1.91	0.21	0	0

A test with a greatly increased value of $\sigma_3 - u$ is the most obvious way of increasing the interparticle contact forces and thus reducing the yield stress at the contacts. Such a test is illustrated in figure 21, the breaks in the curves at the pressure change zones indicating the difficulty of maintaining $(\sigma_3 - u)$ constant while adjusting both σ_3 and u continuously once the range of the self-compensating mercury control was exceeded. Here the value of $(\sigma_3 - u)$ is 6.91 MN/m² (1002.6 lbf/in²) and $\Delta u = 41.4$ MN/m² (6000 lbf/in²).

If we consider the point on the stress–strain curve at which the axial strain is 7.52 %, and the stress difference $(\sigma_1 - \sigma_3) = 12.8$ MN/m² (1852 lbf/in²), then the mobilized value of $\phi' = 28.7°$. Proceeding as before, and considering only the cases with junction growth, we obtain the values given in table 4. Since the value of $(\sigma_n - u)$ on the failure surface is now 10.2 MN/m² and is thus 18 times larger than in the test discussed above, the interparticle contact force might be expected to correspond to a contact area mid-way between the limiting values. The absence of a step in the stress–strain curve would then constitute strong evidence against the validity of the intergranular stress equation (2), and significant evidence against Skempton's effective stress equation (5).

However, samples of Ham River sand sheared at this stress level (i.e. 6.9 MN/m²) show a substantial degree of particle crushing as the shear strain increases. The change in particle size distribution observed in an earlier series of tests and described by Bishop (1966) is illustrated in figure 22. While it is difficult to quantify the effect of particle fracture on the average interparticle force, it will clearly involve a substantial reduction. The prediction of the influence of pore pressure change using Skempton's equation thus returns to the range of values where discrimination is difficult, unless the magnitude of the pore pressure change is increased to a value well beyond the range of the present equipment.

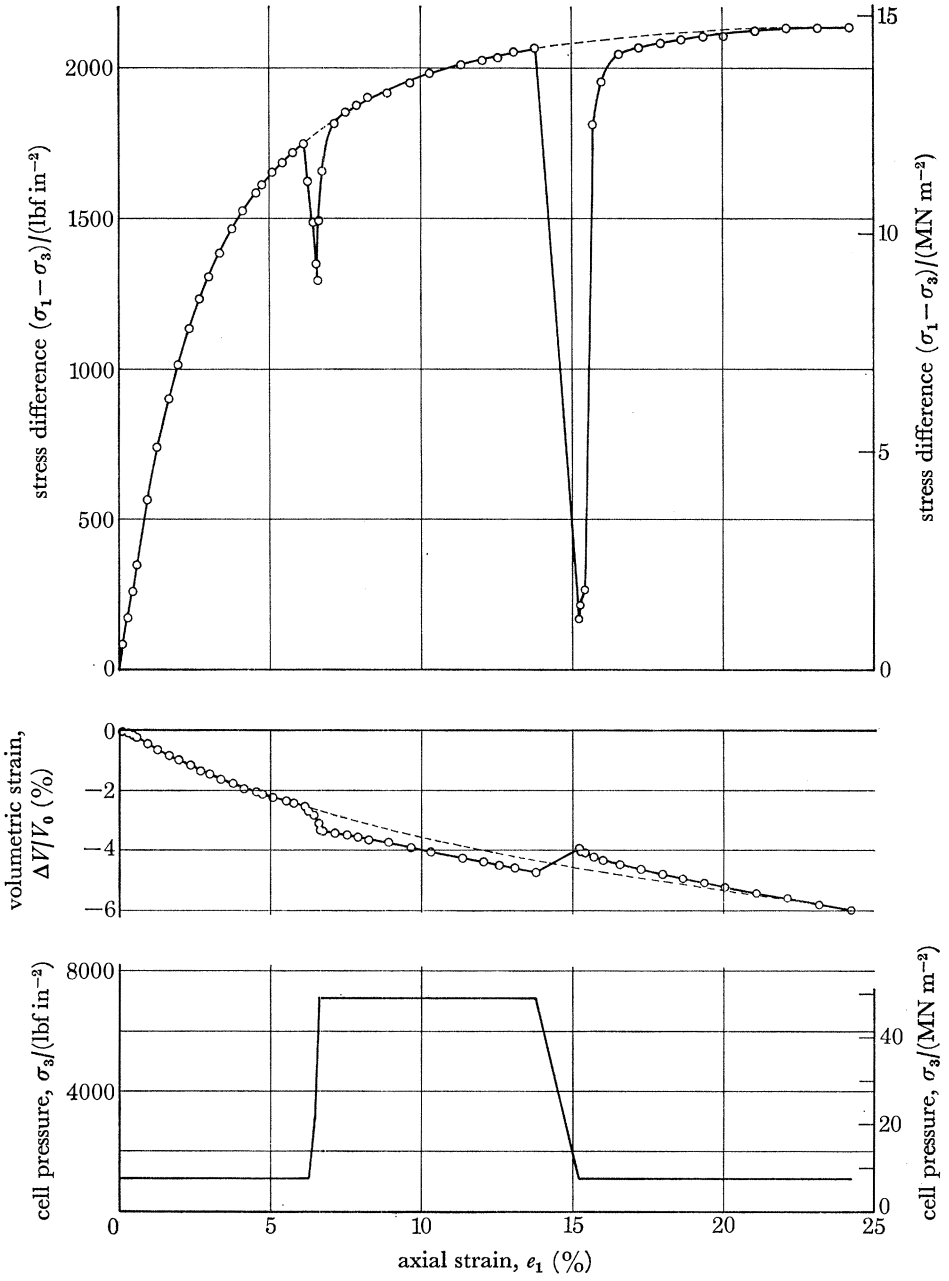

FIGURE 21. Ham River sand tested with (σ_3-u) = 6.91 MN m^{-2} (1002.6 lbf in^{-2}).

TABLE 4. PREDICTED CHANGES IN STRENGTH FOR A CHANGE IN PORE PRESSURE Δu = 41.4 MN/m^2, THE VALUE OF (σ_3-u) BEING CONSTANT AND EQUAL TO 6.91 MN/m^2; HAM RIVER SAND

		intergranular stress equation (2)		Skempton's effective stress equation (5)		Terzaghi effective stress equation (1)	
assumption about contact area a	value of a	$\Delta(\sigma_1-\sigma_3)_f$ kN/m^2	$\frac{\Delta(\sigma_1-\sigma_3)_f}{(\sigma_1-\sigma_3)_f}$ (%)	$\Delta(\sigma_1-\sigma_3)$ kN/m^2	$\frac{\Delta(\sigma_1-\sigma_3)_f}{(\sigma_1-\sigma_3)_f}$ (%)	$\Delta(\sigma_1-\sigma_3)$ kN/m^2	$\frac{\Delta(\sigma_1-\sigma_3)_f}{(\sigma_1-\sigma_3)_f}$ (%)
with junction growth, max. probable value	5.53×10^{-3}	423	3.31	225	1.76	0	0
with junction growth, value corresponding to load of 2 gf per contact	1.18×10^{-3}	90	0.71	48	0.38	0	0

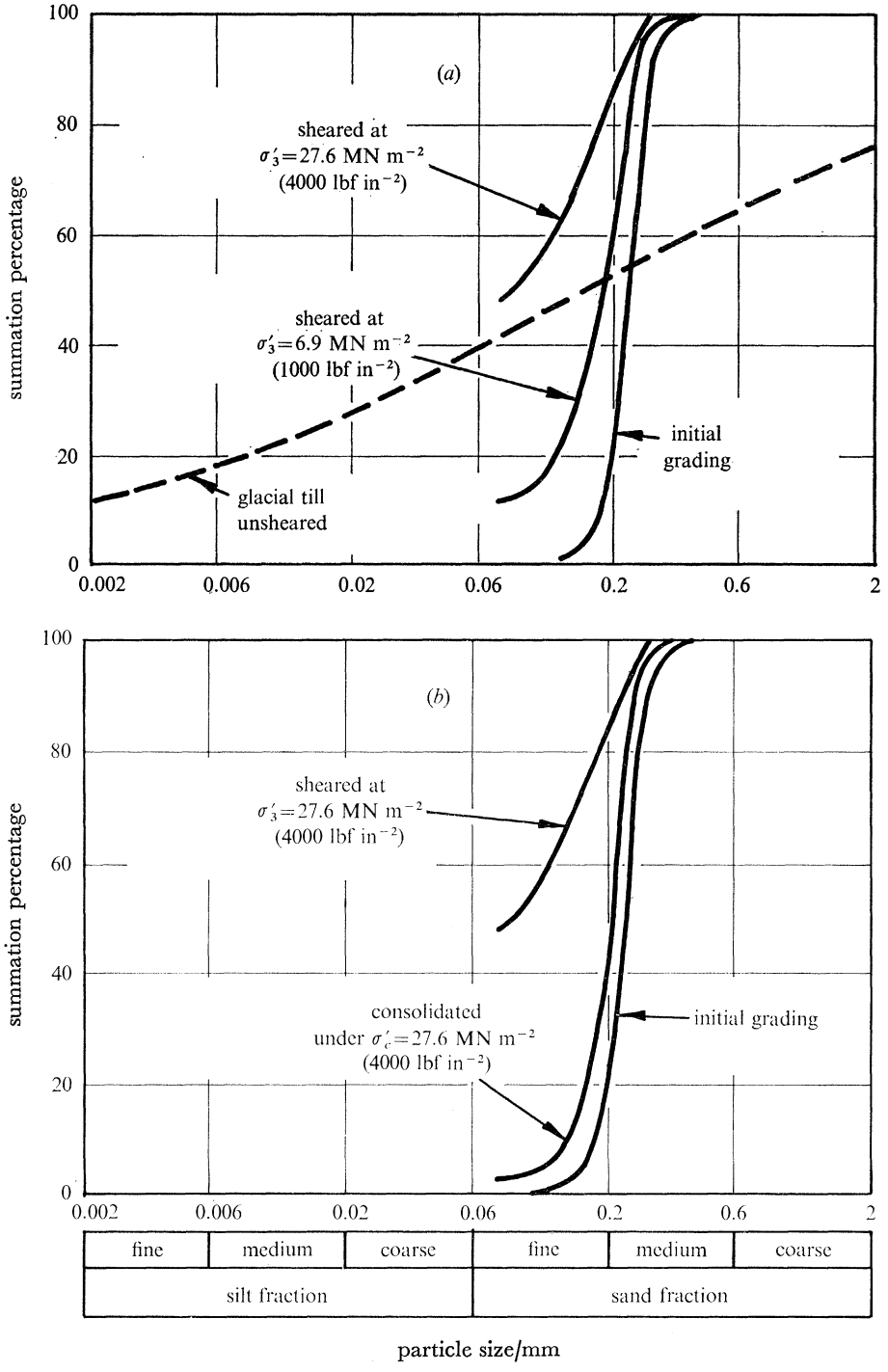

FIGURE 22. Changes in grading of saturated samples of Ham River sand resulting (*a*) from shear at different pressures and (*b*) from consolidation as compared with complete shear tests (tests by Skinner, 1964–66).

(*b*) *Lead shot*

Owing to the low yield stress of lead, this material offered the prospect of definitive results at relatively modest stress levels. The results of a test run in the high pressure apparatus with $(\sigma_3 - u)$ equal to 363 kN/m² (52.6 lbf/in²) and a variation of σ_3 between 1.03 MN/m² (150 lbf/in²) and 27.58 MN/m² (4000 lbf/in²) are shown in figure 23. Once again, there is no discernible change in shearing resistance resulting from a change in pore pressure of 26.5 MN/m² (3850 lbf/in²) with $(\sigma_3 - u)$ held constant.

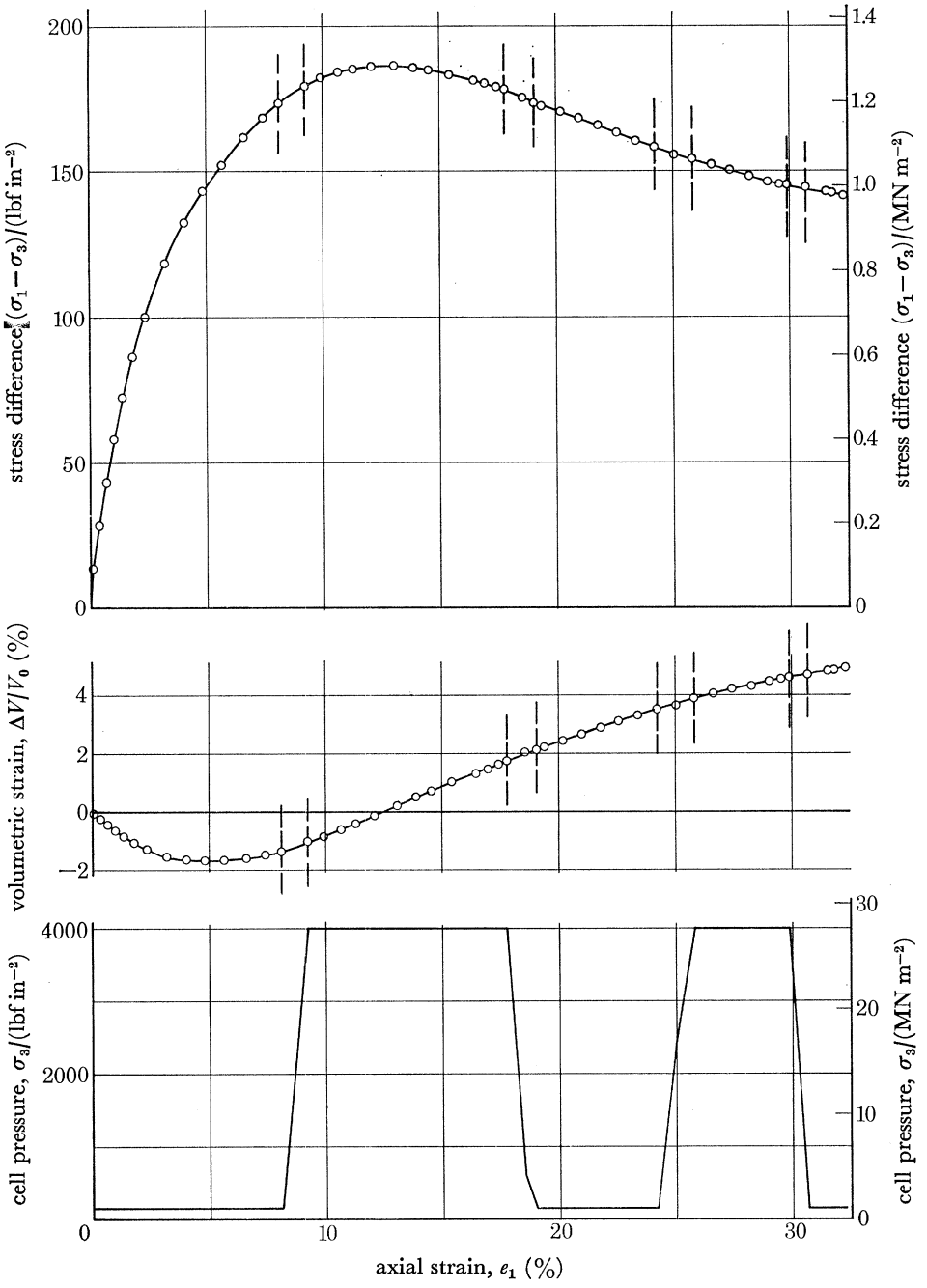

FIGURE 23. Lead shot tested with $(\sigma_3 - u)$ = 363 kN m^{-2} (52.6 lbf in^{-2}).

The area of contact may be derived by three independent methods. Skempton (1960) gives the values of the intrinsic parameters k and ψ for lead as 9.81 MN/m² (100 kgf/cm²) and $\frac{3}{4}°$ respectively. Taking the value of $(\sigma_n - u)$ at an axial strain of 9.24 % as 591 kN/m² we obtain a value of contact area a of 2.97 % using Skempton's expression (equation (13)). For $b = 1$ the same value is obtained from equation (12), but with $b = 3$, which seems more appropriate in the light of values obtained on other metals by Bowden & Tabor (1954), the value of a drops to 0.991 %.

Micro-indentation hardness tests on representative lead shot from this series of tests gave a mean normal stress H_v of 93.1 MN/m² (950 kgf/cm²). On the assumption that $H_v = 3$, $S = 6$ Mk, this value corresponds to $k = 15.3$ MN/m² and suggests a slightly stronger material than the lead quoted by Skempton. Taking the contact pressure as approximating to the indentation hardness value we obtain a value of $a = 0.635$ %. The low value of coefficient of friction (0.1) measured in direct observations of interparticle friction (Skinner 1975) suggests that friction is controlled by surface films on the lead and that junction growth is not very significant in this case.

TABLE 5. VALUES OF CONTACT AREA a FROM OEDOMETER TESTS ON LEAD SHOT†

vertical pressure p in oedometer		value of contact area a on release of stress
MN/m²	kgf/cm²	
2.65	27	0.03
12.55	128	0.11
100.42	1024	0.95

† Data from Laughton (1955).

Thirdly, Laughton (1955) measured with a microscope the facets caused by subjecting lead shot to a series of normal stresses in an oedometer. Since these facets represent the inelastic component of deformation, they indicate the minimum values of a. Laughton's observations, which are also quoted by Skempton (1960), are presented in table 5. It will be seen that up to a contact area of 11 % the relation between a and the vertical pressure p is almost linear and is given by the expression

$$a = 0.0120p(1 - 0.0216p), \tag{32}$$

where p is expressed in MN/m².

In the oedometer the vertical pressure p is applied through a piston and the sample is confined in a rigid-walled cylinder. The radial stress, neglecting side friction, is equal to $K_0 p$, where K_0 is the coefficient of earth pressure at rest and approximates numerically to $(1 - \sin\phi')$ on first loading (Jaky 1948; Bishop 1958). Laughton did not examine the variation of contact area with the direction of the plane of reference and the average contact area measured will therefore correspond to a normal stress of $\frac{1}{3}(1 + 2K_0)\,p$.

In the present test the peak value of $\phi' = 39.7°$ and the equivalent normal stress σ is related to p by the expression

$$\sigma = 0.573p. \tag{33}$$

For the value of $(\sigma_n - u) = 591$ kN/m² we thus obtain $a = 1.21$ %. It is of interest to note the relatively close agreement of this direct experimental value with the values deduced from equation (12) with $b = 3$ and from the micro-indentation hardness tests, having regard to the fact that they refer to different samples of lead.

The magnitudes of the predicted changes in strength for this particular test are given in table 6. It will be seen that the intergranular stress equation predicts an increase in strength, for the

TABLE 6. PREDICTED CHANGES IN STRENGTH FOR A CHANGE IN PORE PRESSURE $\Delta u = 26.5$ MN/m², THE VALUE OF $(\sigma_3 - u)$ BEING CONSTANT AND EQUAL TO 0.363 MN/m²; LEAD SHOT

		intergranular stress equation (2)		Skempton's effective stress equation (5)		Terzaghi effective stress equation (1)	
assumption about contact area a	value of a	$\frac{\Delta(\sigma_1-\sigma_3)_f}{\text{kN/m}^2}$	$\frac{\Delta(\sigma_1-\sigma_3)_f}{(\sigma_1-\sigma_3)_f}$ (%)	$\frac{\Delta(\sigma_1-\sigma_3)_f}{\text{kN/m}^2}$	$\frac{\Delta(\sigma_1-\sigma_3)_f}{(\sigma_1-\sigma_3)_f}$ (%)	$\frac{\Delta(\sigma_1-\sigma_3)_f}{\text{kN/m}^2}$	$\frac{\Delta(\sigma_1-\sigma_3)_f}{(\sigma_1-\sigma_3)_f}$ (%)
without junction growth with $b = 3$, using Skempton (1960) values of k and ψ	0.991×10^{-2}	894	72.3	14.4	1.17	0	0
without junction growth, using results of micro-indentation test	0.635×10^{-2}	573	46.4	9.24	0.75	0	0
using interpretation from Laughton (1955) experimental values	1.21×10^{-2}	1091	88.3	17.6	1.42	0	0

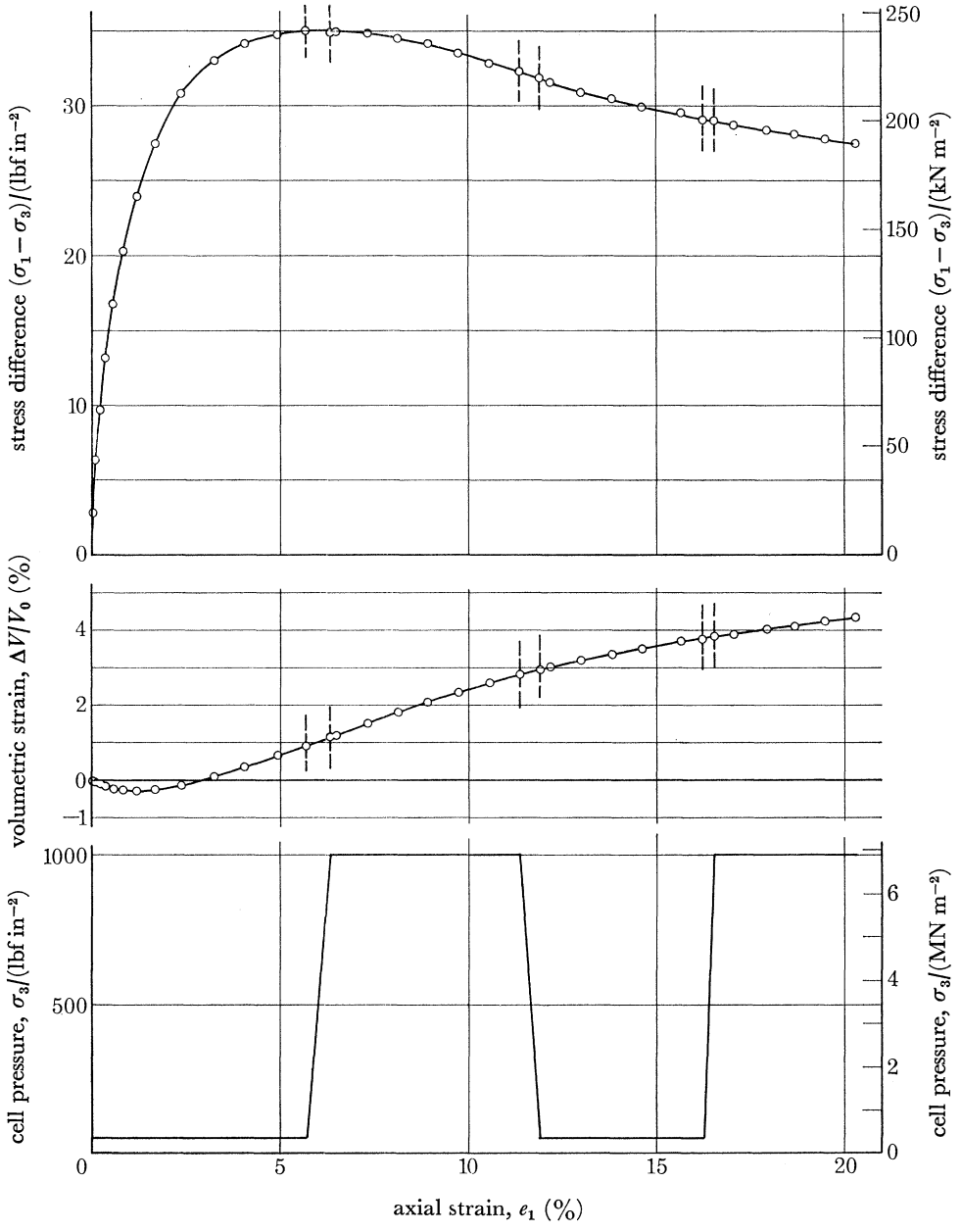

FIGURE 24. Crushed marble tested with $(\sigma_3 - u) = 69.0$ kN m^{-2} (10 lbf in^{-2}).

specified increase in pore pressure, of between 46.4 % and 88.3 %, whereas no detectable increase can be observed in figure 23. The validity of this equation is thus undisputably disproved. Skempton's effective stress equation predicts an increase of between 0.75 % and 1.42 %, and, though much less at variance with the observed stress–strain curve, must be considered to be significantly inconsistent with the experimental result.

Only the Terzaghi equation predicts to within the accuracy of the experimental observations.

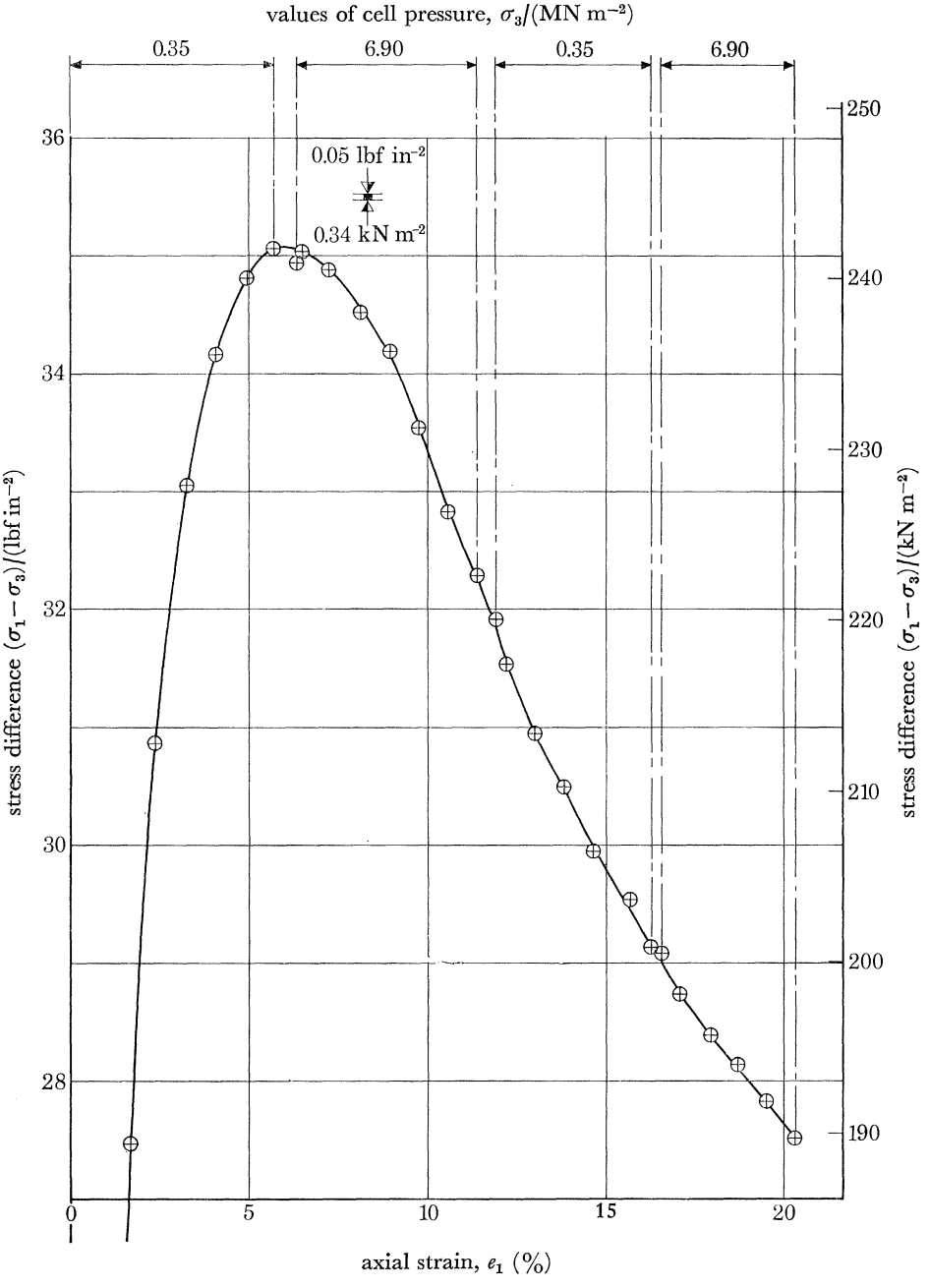

FIGURE 25. Crushed marble – an enlargement of the critical part of the stress–strain curve shown in figure 24.

(c) *Crushed marble*

Part of the testing facilities required for the high pressure cell was in use on another project at this stage of the programme, and the multistage test on crushed marble was therefore carried out in the 0–6.9 MN/m² capacity cell. Particular care was therefore taken to eliminate stray sources of scatter from the values defining the stress–strain curve.

The test was run with $(\sigma_3 - u)$ equal to 68.9 kN/m² (10.0 lbf/in²) and a variation of σ_3 between 349 kN/m² (50 lbf/in²) and 6.895 MN/m² (1000 lbf/in²). The test results are presented in figure 24 and the critical section of the stress–strain curve is given to an enlarged scale in figure 25. Inspection of the curve in figure 25 suggests that any consistent jump in the curve of more that 0.34 kN/m² (0.05 lbf/in²) would be readily discerned, i.e. a jump of 0.14 %.

TABLE 7. PREDICTED CHANGES IN STRENGTH FOR A CHANGE IN PORE PRESSURE $\Delta u = 6.55$ MN/m², THE VALUE OF $(\sigma_3 - u)$ BEING CONSTANT AND EQUAL TO 68.9 kN/m²; CRUSHED MARBLE

		intergranular stress equation (2)		Skempton's effective stress equation (5)		Terzaghi effective stress equation (1)	
assumption about contact area a	value of a	$\frac{\Delta(\sigma_1-\sigma_3)_f}{\text{kN/m}^2}$	$\frac{\Delta(\sigma_1-\sigma_3)_f}{(\sigma_1-\sigma_3)_f}$ (%)	$\frac{\Delta(\sigma_1-\sigma_3)_f}{\text{kN/m}^2}$	$\frac{\Delta(\sigma_1-\sigma_3)_f}{(\sigma_1-\sigma_3)_f}$ (%)	$\frac{\Delta(\sigma_1-\sigma_3)_f}{\text{kN/m}^2}$	$\frac{\Delta(\sigma_1-\sigma_3)_f}{(\sigma_1-\sigma_3)_f}$ (%)
without junction growth, and with $b = 1$	2.63×10^{-4}	6.04	2.50	1.03	0.43	0	0
without junction growth, and with $b = 3$	8.78×10^{-5}	2.02	0.84	0.34	0.14	0	0
with junction growth, probable value	3.39×10^{-4}	7.78	3.22	1.32	0.55	0	0

The predicted values are based on two sets of data. The intrinsic parameters k and ψ may be assumed to approximate to those of calcite given by Skempton (1960) as 186.3 MN/m² (1900 kgf/cm²) and 8° respectively. Taking the value of $(\sigma_n - u)$ at an axial strain of 5.69 % as 112.85 kN/m² we obtain a value of the contact area a of 0.0263 %, using Skempton's expression (equation (13)). For $b = 1$ the same value is obtained from equation (12), but with $b = 3$ this value would fall to 0.00878 %. Micro-indentation hardness tests on the actual material gave a value of $H_v = 2.354$ MN/m². The value of the coefficient of friction μ may then be obtained from the relationship obtained by Skinner (1975):

$$\mu = \tan\psi + \frac{k}{H_v \sin\psi}. \tag{34}$$

This gives a value of 0.7, which is close to the range of values obtained for calcite under saturated conditions by Horn & Deere (1962), namely 0.6–0.68.

Assuming junction growth as in the case of quartz sand we obtain a value of σ_{nj} of 330.0 MN/m² and thus a value of $a = 112.85 \div 333.0 \times 10^3$ (= 0.0339 %). The results of micro-indentation hardness tests on calcite by Brace (1963) indicate that the effect of the magnitude of interparticle force is in this case relatively unimportant.

The magnitudes of the predicted changes in strength on the basis of these contact areas are given in table 7. The validity of intergranular stress equation is again disproved. Skempton's effective stress equation, assuming junction growth, predicts a jump of about four times the minimum magnitude which could be detected, and must therefore be considered to be signifi-

cantly at variance with the experimental results. The Terzaghi equation again gives a correct prediction.

(*d*) *Braehead silt*

Two multistage tests were carried out on Braehead silt in the 0–6.9 MN/m² capacity cell with $(\sigma_3 - u)$ equal to 68.9 kN/m² (10.0 lbf/in²) and a variation of σ_3 between 349 kN/m² (50 lbf/in²) and 6.895 MN/m² (1000 lbf/in²). The results are presented in figures 26 and 27. Inspection of the curves does not show any significant change in shearing resistance following the changes in pore pressure.

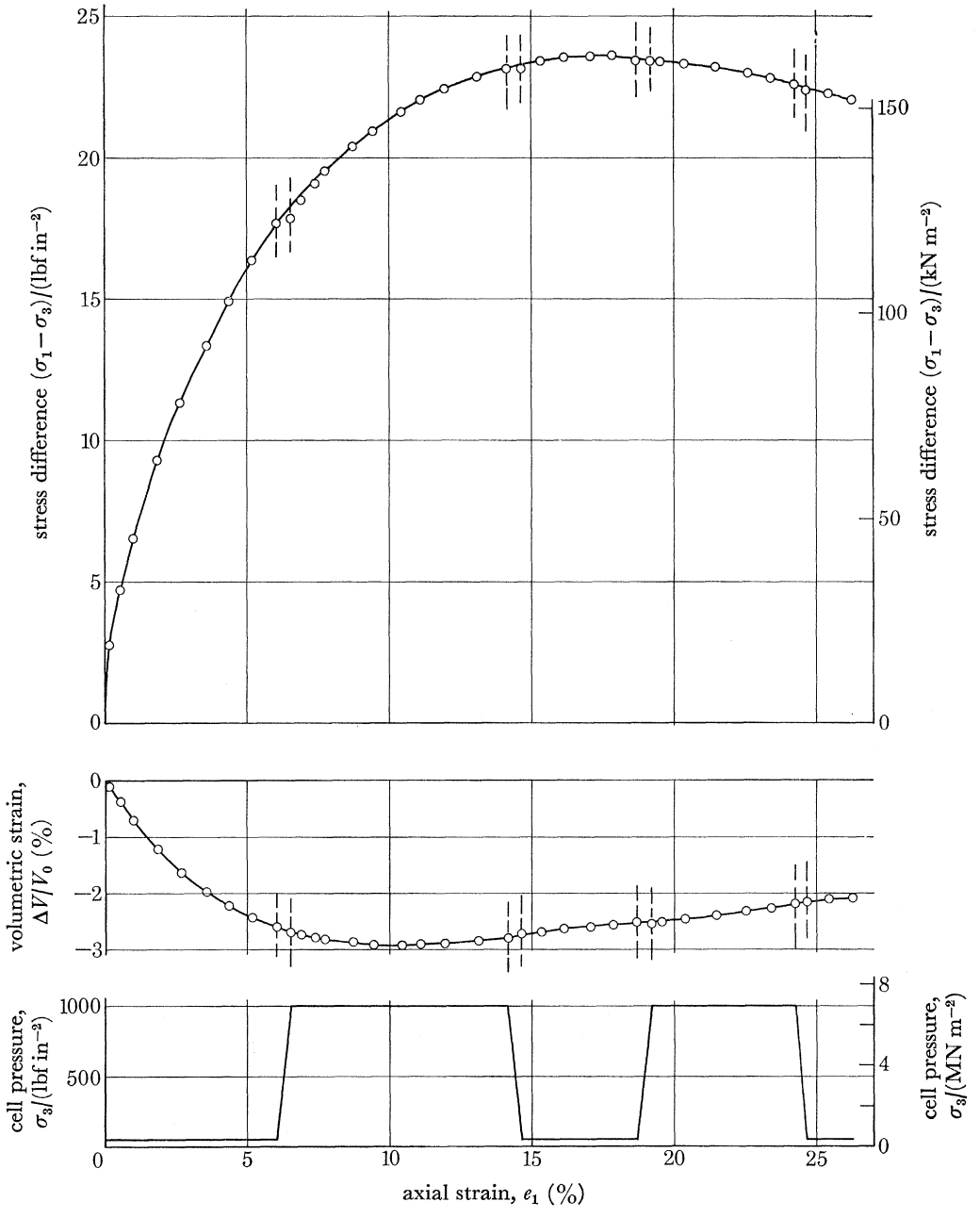

FIGURE 26. Braehead silt tested with $(\sigma_3 - u)$ = 69.0 kN m^{-2} (10 lbf in^{-2}).

The theoretical prediction of the magnitude of strength changes on the basis of the two equations involving the magnitude of the contact area a is subject to some uncertainty, as the predominant mineral is quartz and the average interparticle force is now at least two orders of magnitude smaller than the minimum load used in the micro-indentation tests by Brace (1963). In the absence of the data for evaluating σ_{nj}, table 8 (which refers to the test in figure 27 at 15 % strain) is restricted to estimates based on equations (12) and (13), which do not take account of junction growth or of the magnitude of the interparticle force. However, these values serve to show that a pore pressure change of this magnitude (6.55 MN/m²) is insufficient to provide

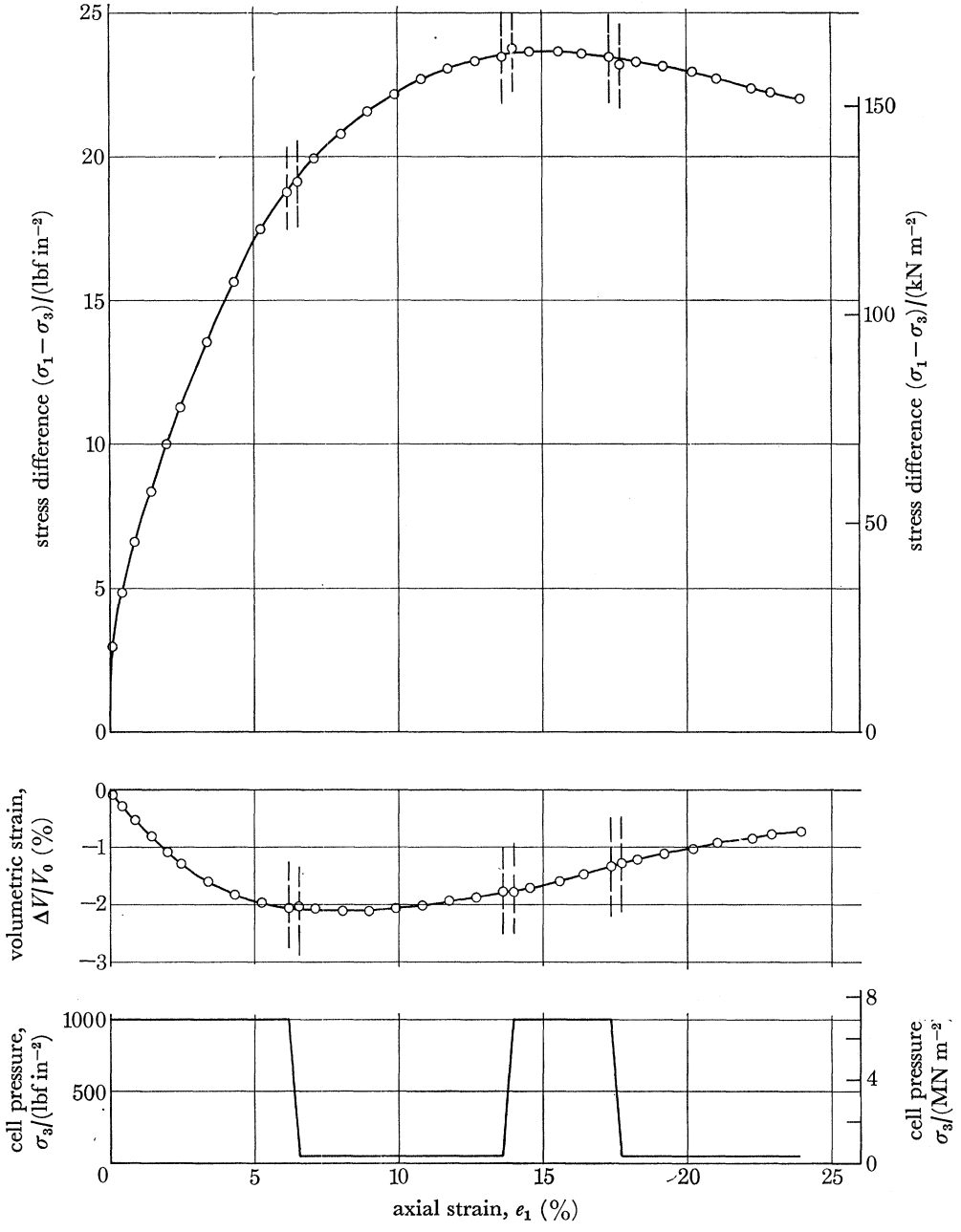

FIGURE 27. Braehead silt tested with (σ_3-u) = 69.0 kN m^{-2} (10 lbf in^{-2}).

critical data for discriminating between the different theories in the case of materials composed predominantly of quartz particles.

The test results, however, do serve to indicate that no other physical phenomenon of greater significance than the interparticle contact area effect enters into the effective stress relationship as the particle size decreases and the material begins to show plasticity in the sense indicated by the Atterberg limits (the *liquid limit* being 29 % and the *plastic limit* 23 %).

TABLE 8. PREDICTED CHANGES IN STRENGTH FOR A CHANGE IN PORE PRESSURE $\Delta u = 6.55$ MN/m², THE VALUE OF $(\sigma_3 - u)$ BEING CONSTANT AND EQUAL TO 68.9 kN/m²; BRAEHEAD SILT

		intergranular stress equation (2)			Skempton's effective stress equation (5)			Terzaghi effective stress equation (1)		
assumption about contact area a	value of a	$\frac{\Delta(\sigma_1-\sigma_3)_f}{\text{kN/m}^2}$	$\frac{\Delta(\sigma_1-\sigma_3)_f}{(\sigma_1-\sigma_3)_f}$	(%)	$\frac{\Delta(\sigma_1-\sigma_3)_f}{\text{kN/m}^2}$	$\frac{\Delta(\sigma_1-\sigma_3)_f}{(\sigma_1-\sigma_3)_f}$	(%)	$\frac{\Delta(\sigma_1-\sigma_3)_f}{\text{kN/m}^2}$	$\frac{\Delta(\sigma_1-\sigma_3)_f}{(\sigma_1-\sigma_3)_f}$	(%)
without junction growth, and with $b = 1$	4.24×10^{-5}	0.66	0.40		0.30	0.19		0	0	
without junction growth, and with $b = 3$	1.41×10^{-5}	0.22	0.13		0.10	0.06		0	0	

6. CONCLUSIONS

The experimental results demonstrate, with a greater degree of accuracy than has been achieved in any previous investigation, the validity of the principle of effective stress as applied to the shear strength of cohesionless particulate materials. The results indicate that for the range of effective stresses and pore pressure changes investigated the principle of effective stress can be expressed to a high degree of accuracy by the simple Terzaghi equation $\sigma' = \sigma - u$. For the Ham River sand the maximum value of the minor principal effective stress was 6.91 MN/m² (1002.6 lbf/in²) and the maximum change in pore water pressure was 41.4 MN/m² (6000 lbf/in²) which is equivalent to a height of 4.2 km of water.

The investigation also demonstrates quite clearly that the often-made assumption that shear strength is controlled by the intergranular stress is invalid. In the case of lead shot this assumption would have led to gross errors of the order of 46–88 % and here there can be little doubt about the magnitude of the contact area a.

The expression derived by Skempton (1960) to take account of the intrinsic angle of friction of the solid material forming the particles gives a significantly less satisfactory agreement with the experimental data than the Terzaghi equation for lead shot and for calcite. For quartz sand the conclusion to be drawn is less clear, owing to the probable sensitivity of the value of the contact area a at a given value of $(\sigma_n - u)$ to the magnitude of the interparticle force. Changes in pore pressure an order of magnitude greater than were used in the present series of tests would be necessary to give a really convincing demonstration of the status of this expression for hard particles such as quartz. However, in as far as the expression predicts jumps in the stress–strain curve as indicated in tables 3 and 4, it is not supported by any positive evidence.

One reason for the apparent lack of validity of Skempton's expression for effective stress may be its dependence on the Caquot–Bishop–Horne type of relation between ϕ' and the coefficient of interparticle friction μ. More recent work (Skinner 1969 and 1975, and unpublished radiographic work) indicates that the mechanism of failure in random particulate materials is more complex than assumed in any current analysis and that no unique $\phi' - \mu$ relation exists. A rigorous analytical solution to this problem is not yet forthcoming.

PHILOSOPHICAL TRANSACTIONS OF THE ROYAL SOCIETY A MATHEMATICAL, PHYSICAL & ENGINEERING SCIENCES

The only data available in 1960 for studying the influence of contact area on the strength of porous materials subject to high pore-water pressures was from tests on strongly cohesive materials such as intact marble, limestone and concrete. The critical data (Skempton 1960) was provided by unjacketed samples (in which $\sigma_3 - u = 0$) tested under a range of cell pressures in rather cruder apparatus than used in the present series of tests. Unjacketed samples are subject to brittle failure at small strains, cohesion making the main contribution to compression strength. In the authors' view more relevant data would be obtained by running constant $(\sigma_3 - u)$ tests in the pressure range in which plastic failure occurs (for example $\sigma_3 - u = 50$–$70\,\mathrm{MN/m^2}$ on the basis of Karman's (1911) classic tests on marble). Here friction plays a more important part in the resistance to shear (whether considered in terms of the Mohr–Coulomb or the modified Griffith failure criterion (see, for example, McClintock & Walsh 1962; Hoek 1965)) and the shape of the stress–strain curve is sufficiently flat-topped to permit multistage tests, with due allowance in the rate of strain for the low permeability of the sample.

The early stages of the investigation were supported by the Department of Scientific and Industrial Research and by the Civil Engineering Research Association (now S.R.C. and C.I.R.I.A. respectively). Mr F. Winser contributed to the success of the experimental investigation by very high precision work on the high pressure cells and Mr David Evans assisted in the assembly of the various pressure systems.

References

Aldrich, M. J. Jr. 1969 Pore pressure effects on Berea Sandstone subjected to experimental deformation. *Bull. Am. Geol. Soc.* **80**, 1577–1586.

Bishop, A. W. 1953 (Private communication to Dr A. S. Laughton) (see Skempton 1960).

Bishop, A. W. 1954 Correspondence on shear characteristics of a saturated silt, measured in triaxial compression. Penman, A. D. M. (Geotechnique, 3, No. 8, 312–328). Letter to Geotechnique. *Geotechnique* **4**, 43–45.

Bishop, A. W. 1955 Lecture delivered in Oslo, entitled 'The principle of effective stress'. Printed in *Teknisk Ukeblad, No.* 39 (1959), 859–863.

Bishop, A. W. 1958 Test requirements for measuring the coefficient of earth pressure at rest. *Proc. Brussels Conf. Earth Pressure Problems* **1**, 2–14.

Bishop, A. W. 1965 Discussion. *Proc. 6th Int. Conf. Soil Mech.* **3**, 306–310.

Bishop, A. W. 1966 Strength of soils as engineering materials. 6th Rankine Lecture. *Geotechnique* **16**, 89–130.

Bishop, A. W. 1969 Discussion. *Proc. 7th Int. Conf. Soil Mech.* **3**, 182–186.

Bishop, A. W. 1973 The influence of an undrained change in stress on the pore pressure in porous media of low compressibility. (Technical note.) *Geotechnique* **23**, 435–442.

Bishop, A. W. & Blight, G. E. 1963 Some aspects of effective stress in saturated and partly saturated soils. *Geotechnique* **13**, 177–197.

Bishop, A. W. & Eldin, A. K. G. 1950 Undrained triaxial tests in saturated sands and their significance in the general theory of shear strength. *Geotechnique* **2**, 13–32.

Bishop, A. W. & Henkel, D. J. 1962 *The measurement of soil properties in the triaxial test*, 2nd ed. London: Edward Arnold.

Bishop, A. W., Kumapley, N. K. & El-Ruwayih, A. 1975 The influence of pore-water tension on the strength of clay. *Phil. Trans. R. Soc. Lond.* A **278**, 511–554.

Bishop, A. W., Webb, D. L. & Skinner, A. E. 1965 Triaxial tests on soil at elevated cell pressures. *Proc. 6th Conf. Soil Mech.* **1**, 170–174.

Bowden, F. P. & Tabor, D. 1942 Mechanism of metallic friction. *Nature, Lond.* **150**, 197–199.

Bowden, F. P. & Tabor, D. 1950 *The friction and lubrication of solids. Part I.* Oxford University Press.

Bowden, F. P. & Tabor, D. 1954 *The friction and lubrication of solids. Part I.* Corrected impression. Oxford University Press.

Bowden, F. P. & Tabor, D. 1964 *The friction and lubrication of solids. Part II.* Oxford University Press.

Brace, W. F. 1963 Behaviour of Quartz during indentation. *J. Geol.* **71**, 5, 581–595.

Bruggeman, J. R., Zangar, C. N. & Brahtz, J. H. A. 1939 Memorandum to Chief Designing Engineer: notes on analytic soil mechanics. *U.S. Dept. of the Interior, Tech. Mem.*, No. 592.

PHILOSOPHICAL TRANSACTIONS OF THE ROYAL SOCIETY A MATHEMATICAL, PHYSICAL & ENGINEERING SCIENCES

Caquot, A. 1934 *Equilibre des Messifs à Frottement Interne, Pulvérulents et Cohérentes.* Paris: Gauthier-Villars.
Hoek, E. 1965 Rock fracture under static stress conditions. Ph.D. thesis, University of Capetown. *CSIR Report MEG 383*, Pretoria, South Africa.
Horn, H. M. & Deere, D. U. 1962 Frictional characteristics of minerals. *Geotechnique* **12**, 319–335.
Horne, M. R. 1969 The behaviour of an assembly of rotund rigid, cohesionless particles. III. *Proc. R. Soc. Lond.* A **310**, 21–34.
Hubbert, M. K. & Rubey, W. W. 1959 Rôle of fluid pressure in mechanics of overthrust faulting. *Bull. Am. Geol. Soc.* **70**, 115–206.
Jaky, J. 1948 Pressure in silos. *Proc. 2nd Int. Conf. Soil Mech.* **1**, 103–107.
Karman, Th. von. 1911 Festigkeitsversuch unter allseitigem Druck. *Ziet. Vereines Deutsch, Ing.* **55**, 1749–1757.
Laughton, A. S. 1955 The compaction of ocean sediments. Ph.D. thesis. University of Cambridge.
McClintock, F. A. & Walsh, J. B. 1962 Friction on Griffith cracks under pressure. *4th U.S. Nat. Congress of Appl. Mech. Proc.* 1015–1021.
Procter, D. C. & Barton, R. R. 1974 Measurements of the angle of interparticle friction. *Geotechnique* **24**, 581–604.
Scott, R. F. 1963 *Principles of soil mechanics.* Addison Wesley.
Skempton, A. W. 1960 Effective stress in soils, concrete and rocks. *Conf. on Pore Pressure and Suction in Soils.* London: Butterworths.
Skinner, A. E. 1969 A note on the influence of interparticle friction on the shearing strength of a random assembly of spherical particles. *Geotechnique* **19**, 150–157.
Skinner, A. E. 1975 The effect of high pore water pressures on the mechanical behaviour of sediments. Ph.D. thesis, University of London.
Taylor, D. W. 1944 Cylindrical compression research program on stress-deformation and strength characteristics of soils. *M.I.T. 10th Progress Report to U.S. Engineers Department.*
Taylor, D. W. 1948 *Fundamentals of soil mechanics.* New York: John Wiley.
Terzaghi, K. 1923 Die Berechnung der Durchlässigkeits-Ziffer des Tones aus dem Verlauf der hydrodynamischen Spannungserscheinungen. *Sitz. Akad. Wissen. Wien Math-naturw. Kl. Abt. IIa* **132**, 125–138.
Terzaghi, K. 1925 *Erdbaumechanik auf bodenphysikalischer Grundlage.* Leipzig: Deuticke.
Terzaghi, K. 1936 The shearing resistance of saturated soils and the angle between the planes of shear. *Proc. 1st Int. Conf. Soil Mech.* **1**, 54–56.
Tombs, S. G. 1969 Strength and deformation characteristics of rockfill Ph.D. thesis, University of London.

PHILOSOPHICAL TRANSACTIONS OF THE ROYAL SOCIETY A MATHEMATICAL, PHYSICAL & ENGINEERING SCIENCES

FIGURE 6. (a) 6.90 MN m^{-2} triaxial apparatus. (b) 68.95 MN m^{-2} triaxial cell.